Rockefeller University
Digital Commons @ RU

Student Theses and Dissertations

2015

Hair Bundles of a Jawless Vertebrate Employ Tetrapod-Like Tuned Mechanical Amplification

Katherine J. Leitch

Follow this and additional works at: http://digitalcommons.rockefeller.edu/student_theses_and_dissertations

 Part of the Life Sciences Commons

Recommended Citation

Leitch, Katherine J., "Hair Bundles of a Jawless Vertebrate Employ Tetrapod-Like Tuned Mechanical Amplification" (2015). *Student Theses and Dissertations.* Paper 271.

This Thesis is brought to you for free and open access by Digital Commons @ RU. It has been accepted for inclusion in Student Theses and Dissertations by an authorized administrator of Digital Commons @ RU. For more information, please contact mcsweej@mail.rockefeller.edu.

HAIR BUNDLES OF A JAWLESS VERTEBRATE EMPLOY TETRAPOD-LIKE TUNED MECHANICAL AMPLIFICATION

A Thesis Presented to the Faculty of

The Rockefeller University

in Partial Fulfillment of the Requirements for

the degree of Doctor of Philosophy

by

Katherine J. Leitch

June 2015

© Copyright by Katherine J. Leitch 2015

HAIR BUNDLES OF A JAWLESS VERTEBRATE EMPLOY TETRAPOD-LIKE TUNED MECHANICAL AMPLIFICATION

Katherine J. Leitch, Ph.D.

The Rockefeller University 2015

In the hearing and balance organs of tetrapod vertebrates, mechanical signals are transduced by an elegant organelle called the hair bundle. Deflections of this structure apply forces to mechanically gated ion channels. Hair bundles are not passive receivers of stimuli, but are instead active participants in the process of sensory transduction. They expend chemical energy to exert mechanical work, and can harness this active process to amplify their mechanical response to stimuli. Furthermore, the active process is tuned, allowing a given hair bundle to preferentially amplify a particular frequency; this feature is valuable in the analysis of complex sounds. Hair bundles can also enter an unstable regime in which their active process drives spontaneous oscillations. Studying this epiphenomenon can reveal mechanisms underlying the amplifying abilities of hair bundles.

Despite the importance of amplification in hearing, little is known regarding the evolution of the active process; it is unclear if the active process is exclusive to tetrapods. It would be instructive, for instance, to know whether the active process predates the array of auditory specializations seen throughout vertebrates. Here, we approach this problem by investigating the mechanical activity of the hair bundles from the inner ears of two jawless vertebrates, the sea lamprey *Petromyzon marinus* and the American brook

lamprey *Lampetra appendix*. We observe spontaneous oscillations in both of these animals. In the latter species, we also show evidence that their oscillations stem from mechanisms similar to those driving the spontaneous oscillations of tetrapod vertebrates. Furthermore, we found that hair bundles exhibiting these movements can entrain to and mechanically amplify particular stimulus frequencies. Taken together, our findings from a group distantly related to the tetrapods suggest that the active process of hair bundles is trait ancestral to all vertebrate ears.

Acknowledgements

I'd like to thank my advisor, Jim Hudspeth, for providing me the opportunity to pursue this study on lamprey hair cells and for all he has taught me. I continue my scientific career with a profound sense of possibility, and this is largely due to his example. Jim makes things work, end of story - whether expertly dissecting a osteichthyan ear on the first attempt, lifting objects bordering on too-heavy, or protecting in a tiny water droplet the tip of a sharp microelectrode as its shaft is melted and shaped.

My interest in animals and ecosystems I attribute to my parents. Thank you, Mom and Dad, for moving us to Rum Creek and the millpond, where I could spend my summers watching tadpoles metamorphose and catching lamprey. Dad, I appreciate your patience during our early birdwatching trips together; I unleashed a lot of eye-rolling during that period in which species names seemed so pointless to me. (Now I get the point.) Mom, you have given me so much help, and you've been an inspiring role model. Thanks for setting up all those aquaria of gelatin for my volcanic lake experiments. And I will never forget the day that your work schedule conflicted with your monarch's pupation schedule – so you brought him, on his unwieldy milkweed, in to work. I still want to run a lab with you.

I first noticed that I could be a scientist while in Heather Eisthen's lab at Michigan State. Heather believed in me and challenged me. From that era I also must thank Sue and Dick Hill. Sue was deeply kind, and together we spent many afternoons watching *Capitella* in their tubes. Dick's lectures ignited my interest in comparative physiology, especially the topic of camel thermoregulation. George von Dassow and Sveta Maslakova taught a beautiful course that gave me a glimpse, in an array of custard

cups, of the Cambrian Explosion. They also taught me that observing animals has an important place in biology. I have to thank Fred Reusch and Emma Schroder, who together taught me calculus and made high school a happy time, and the late Starlene Williams-Mars, who taught me how to read a scientific paper.

Rudy Bellani and Clare Walton created the Summer Neuroscience Program, and I am so honored that they passed it along to me, Lindsay, and Román. And in turn I am thankful to Aylesse, Laura, Deanna, and Raffi for carrying this torch. Also, thank you to the Dean's Office and to Jeanne Garbarino for supporting this program.

The Hudspeth lab is full of wonderful people, and I thank them all. Particularly I am grateful to Brian for making troubleshooting enjoyable, for taking me just seriously enough, and for being an excellent teacher. I send a slight nod to Aaron, who is a prince of weirdness, a library of knowledge, a loyal friend, and in some sense the lab grandmother. Thanks to Jason for his great suggestion that I work with lamprey. Julien, it has been so nice sharing the orange room and discussing myosins with you. Josh, I appreciate your enthusiasm, insight, and your consistent willingness to help others. Adrian, thanks for your friendship and for saving me from hydrodynamic confusion. Taeryn, thank you for all your patient advice with the confocal and molecular biology. And Beth, thank you for all your encouragement.

Many scientists outside of the Hudspeth lab were instrumental in my education here at Rockefeller. I am very thankful to my committee members, Daniel Kronauer and Leslie Vosshall, for their steady support, encouragement, and scientific insights. Daniel was very good at helping me prioritize my worries – in effect, downgrading most of them. And Leslie gave me thoughtful, strategic pep-talks. I'm also very thankful to Geoff

Manley for the rewarding conversations we've had so far, and for serving on my external committee. Ona Bloom provided me with my first glimpse of a lamprey ear, and Ellen Lumpkin gave helpful advice on planning an exploratory project. Thanks to David Gadsby for the fantastic Membrane Biophysics labs. I'd like to thank Fernando Nottebohm, Wan-Chun Liu, and Tim Gale for facilitating my inspiring visits to the Rockefeller Field Research Center. Thanks to Pascal Martin for advice on hair-bundle mechanics. Thanks to Bill Eberhard, Gilbert Barrantes, and Anita Aisenberg for our work on *Leucauge*. Thanks to Sandy Simon for his wisdom about the nature of science, and for suggesting I visit Charles Nicholson to measure Ca^{2+} in the ear of the lamprey. Thank you, Charles, for your friendship, generosity, mentorship, and for taking seriously my amateur art.

I am extremely grateful for my friends and family. Thank you, Monica, for always being there when I needed you, and for sharing Bailey; Kavi, for your humane, happy perspective on life; Ben, for showing up with wine. Thanks to Tom, Donovan, and Román for that era of shadow puppetry. Josie, Sean, and Sy, I appreciate your sweetness and your suggestion I be more of a "spoiled brat." Lindsay and Rudy, thank you for all your encouragement and friendship. Sergio, thank you for the tiny ecosystems. Gabriel, thank you for your kindness and your careful criticism of my work. Thank you, Stu, for always being the person I looked up to most, for making me feel that building an airplane would be simple. And Hannah, you are so important to me, because you make me excited about the future. And to my husband Román, thank you for always believing in me, inspiring me, and for making our lives fun.

Table of Contents

List of Figures

List of Tables

1. Introduction

1.1. Why study sensory evolution?

Determining the sensory capabilities of a long-extinct animal is difficult. Many structures that would inform this quest are too small or soft to be observed in any but the rarest of fossils (Poinar and Hess, 1982), and of course fossils do not yield to direct physiological assay. But the question can be approached, and the answers are important for understanding the history of animals and ecosystems on our planet (Nilsson, 2009). Furthermore, understanding the evolutionary history of any physiological process can shed light on its modern manifestations. Making comparisons across groups of animals – needed to infer the physiological attributes of an ancestor – can underscore what is fundamental to a process and can help us disentangle the adaptive from the architecturally, developmentally, or phyletically constrained.

1.1.A. Sensory systems drive diversity

Why are there so many songbird species? Why are some frog families especially diverse? Speciation of animal subpopulations can be driven by pre-mating isolation, and in some cases this rift in gene flow is mediated by divergence in courtship displays. There is evidence that the degree of this divergence can be influenced by the range of sensory stimuli interpretable to an animal: the animal's "sensory bandwidth." Between groups of frogs, there is extensive variability in an auditory organ termed the amphibian papilla; in its ancestral state, the papilla hosts only a small field of receptor cells, thought to be tuned to a narrow range of frequencies; in the most derived anuran ear, the papilla is much larger and consists of two separately innervated fields encoding a broader range of frequencies (Lewis, 1981). Knowing mating calls are variable in anurans and that females

prefer the calls of conspecifcs (Blair, 1964; Ryan and Rand, 1995; Pfennig, 2000), it is intriguing to see a correlation between amphibian papillar complexity and speciation rates (Ryan, 1986) (Figure 1.1). It may be that wider auditory bandwidths loosen a constraint on male calls, permitting greater spectral variability among subpopulations' calls. By blunting gene flow between those subpopulations, this would in turn facilitate speciation (Blair, 1964; Richards, 2006).

A causal link between sensory systems and speciation is clearly seen in cichlid fishes of Lake Victoria. Cichlid species often reside in overlapping habitats, and females have been shown to mate preferentially with conspecifics on the basis of males' nuptial coloration alone. Anthropogenic disturbance of nutrients in the lake has imposed a filter on the wavelengths of penetrating light, but only in some regions of the lake. In the murkiest environs populations of fish display, and confer to their laboratory-reared progeny, far duller colors than do their conspecifics in clearer water. This accidental experiment, ongoing since the early 1900s, has shown that narrowing the available sensory bandwidth can affect the processes leading to species divergence (Seehausen et al., 1997).

The effect of sensory abilities on evolution extends to other kingdoms of life. In flowering plants, species with overlapping habitats may be "ethologically isolated" due to the fidelity with which animal pollinators visit one type of flower (Grant, 1949). Although it is thought that pollinators cannot serve as primary drivers of plant speciation (Chittka et al., 1999), pollinator behavior seems to play a key role; in groups of flowering plants, transitions from abiotic to animal-mediated pollination are consistently correlated with an uptick in diversification (Kay and Sargent, 2009). Furthermore, shifts between

pollinator species, each with their particular sensory biases, can drive divergence within a species complex, generating angiosperm "ecotypes" that differ dramatically in scent, morphology, and flowering timing (Peter and Johnson, 2014; Newman et al., 2014). Because present-day diversity stems from rifts in the past, and because animal senses can influence gene flow, understanding today's ecosystems requires understanding the sensory systems of ancestral, long-fossilized animals.

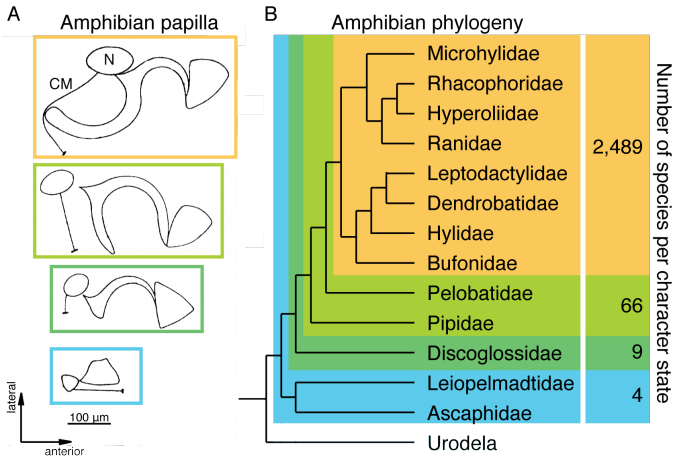

Figure 1.1. Anurans have derived increasingly large, complex amphibian papillae, correlating with the number of species in each group. **A.** The four general states of the amphibian papilla in anurans. N, transected papillar branch of the VIIIth nerve; CM, contact membrane dividing the papillar chamber from the periotic canal. **B.** This color-coded amphibian phylogeny indicates which groups of anurans possess which papillar state. The number of species within each group is noted at far right. Phylogeny not to scale; convergence times of sister groups cannot be read from this diagram. Figure adapted from Ryan (1986); amphibian papilla morphology from Lewis (1981).

1.1.B. Comparisons yield mechanistic insights

Comparing function across extant animals is a fundamental tool of the evolutionary physiologist. When considered in a trusted phylogenetic framework, this information helps us infer ancestral physiological traits. But this act of comparison can also shed light on the mechanisms of modern animals. Teeming with detail, the complexity of a living

animal can frustrate attempts to understand functionality: which of these details are adaptively significant, and which are better understood as byproducts of constraint, or of phyletic inertia (Gould and Lewontin, 1979)? Here, comparing similar systems across taxa can help by drawing our attention to key tissues, cells, organelles, or molecules. This was true in the puzzle of the mammalian kidney. Mammals, unlike most other tetrapod vertebrates, are capable of producing urine that is hyperosmotic to blood plasma, a feat particularly useful when freshwater is scarce. Examining the organ responsible for this, we see that nephrons in the mammalian kidney include hairpin-like segments termed loops of Henle. That these loops are not strikingly homogeneous and are tightly packed amidst convoluted tubules and collecting ducts, gives the viewer an overall impression of spaghetti. For a long time, no researchers queried the physiology of this tangle; where to start? However, in the 1940s Sperber performed a comparative study of mammalian kidneys (reviewed by Hill et al., 2012), grouping the animals into three environmental categories: freshwater, mesic, and arid species. These categories served as a proxy for the presumed selective pressures on urine-concentrating abilities. He found that the renal layer into which particularly long loops of Henle penetrate was by far the thickest in the arid species, suggesting a lengthening of Henle's loops in response to high demands on urine concentration. More recent work directly confirmed this correlation, accounting for body size (Beuchat, 1990). Intrigued, physiologists turned to these loops, eventually showing that their long hairpin structure is instrumental to mammals' production of highly concentrated urine. Specifically, the closely apposed, oppositely oriented flows of the loop drive a countercurrent multiplier effect, concentrating interstitial solutes in the deep layers of the kidney to an extent not thought possible by ion pumps alone (Hargitay

and Kuhn, 2001). Knowing this countercurrent mechanism in the kidney guides efforts to engineer functional kidneys *in vitro* (Chang and Davies, 2012), and unveils an elegant functional analogy between disparate processes: urine concentration in dehydrated desert mammals, heat retention in the swimming muscles of tuna (Carey and Teal, 1966), brain cooling in some mammals (Baker, 1982; Johnsen et al., 1985), and gas transfer in some placentas (Adamson et al., 2002).

This comparative approach, instrumental to advancements in kidney physiology, can also clarify mechanisms of sensory systems. In vertebrates, two similar G-protein-coupled receptors mediate the perception of sweet and umami ligands. Birds lost the vertebrate sweet receptor, raising the question how hummingbirds – specialized nectar feeders – taste sweet compounds. Comparing the genomes of many birds revealed signatures of positive selection on the hummingbird umami receptor; physiological recordings revealed that this receptor had been repurposed to bind sweet ligands. Experimental chimeras of chicken and hummingbird receptors revealed a mere handful of amino acid residues responsible for this dramatic switch in ligand specificity. Thus, not only does this study offer insights into the hummingbird trophic niche, but it also advances our mechanistic understanding of the binding of sweet and umami ligands in all vertebrates (Baldwin et al., 2014).

Comparative studies may prove fruitful in outstanding problems in sensory biology, for example, in the study of magnetoreception. For decades, we have seen a wealth of behavioral evidence for a magnetoreceptive sense in members of all major vertebrate taxa, as well as in arthropods – but we have yet to find the cell type responsible for transducing this stimulus (Lohmann, 2010). For most other sensory modalities,

conspicuous antennae such as auditory pinnae or visual lenses have evolved to collect and modify the stimulus on its way to transducing elements; the curiosity of neurophysiologists is conveniently guided along this same path. Such obvious antennae have not evolved in magnetoreception, perhaps because magnetic fields are unaltered by biological tissue. Moreover, magnetotransduction could theoretically occur through three quite distinct processes, further complicating this search (Johnsen and Lohmann, 2005). Perhaps it will be helpful to compare the nervous systems of many related animals, grouping them by the degree to which their fitness is thought to rely on magnetoreception and allowing adaptive variability to focus our attention.

1.2. Auditory and vestibular mechanoreceptors

Mechanical forces sculpt life. The extraordinary tensile strength of the mussel holdfast reflects the onslaught of waves endured by intertidal organisms (Harrington and Waite, 2007) and developmental processes such as angiogenesis (Ingber, 2002) and neural-tube formation (Odell et al., 1981) are guided by shear forces and tissue tension. But animals are not passively battered; they exploit external forces for their rich information content, thus learning about the immediate and distant environments with a wide variety of mechanoreceptive systems. Touch mechanoreceptors inform animals about objects directly impinging on their bodies, integral to escape responses (Low et al., 2011), navigation (Arkley et al., 2014), object manipulation, and social interactions (Lumpkin et al., 2010). A sense of "distant touch," or near-field hearing, can be achieved by analyzing flows or vibrations in the nearby air, water, or substrate; this sense mediates fish schooling, mosquito and spider courtship (Rovner and Barth, 1981; Cator et al., 2009; Aisenberg and Barrantes, 2011), and parasitoid wasp hunting (Kroder et al., 2006).

Far-field hearing allows for detection and analysis of even more distant stimuli; in this modality, the animal senses pressure fluctuations emanating from, for instance, a conspecific courtship song. Finally, mechanoreceptors in the vestibular system are sensitive to linear and angular accelerations, providing an animal with feedback about its position relative to gravity and about its own motion in space.

1.2.A. Hair cells in vertebrates

In vertebrates, sound and acceleration are sensed by mechanoreceptors called hair cells, so named for their transducing organelle, a cluster of hair-like, actin-filled, apical projections called stereocilia (Figure 1.2 A). Vertebrate hair bundles contain tens to a few hundred stereocilia, in an ordered array displaying height gradation. Mature hair bundles also contain from zero (Jensen-Smith et al., 2003) to two (Lowenstein and Thornhill, 1970) true cilia termed kinocilia. Stereocilia adjoin their neighbors by a variety of proteinacious linkages; one well characterized connection is termed the tip link (Figure 1.2, arrowhead). Upon external forcing, all of the stereocilia pivot about their insertions such that the bundle remains coherent (Karavitaki and Corey, 2010). Deflection of the bundle toward its tallest edge, defined as the positive direction, shears adjacent stereociliary tips with respect to one another (Figure 1.2 B). This tenses a putative gating spring, a component of which is the tip link. As each gating spring's tension increases, so increases the open probability of transduction channels in series with the gating spring (Corey and Hudspeth, 1983). Thus, transduction is direct and fast: mechanical stimuli gate a large cationic conductance (Crawford et al., 1991) without sluggish chemical intermediates. The fastest characterized transduction system mediated by a second messenger, that operating in *Drosophila* photoreceptors, responds to a pulse of light with

a latency of 20 ms (Hardie et al., 2002) and reaches its peak response after about 75 ms (Hardie et al., 2002). In contrast, the hair cells of tetrapod vertebrates display a response latency of merely 40 μs (Corey and Hudspeth, 1983) and their peak transduction current requires less than 5 ms to evolve (Ricci et al., 2000).

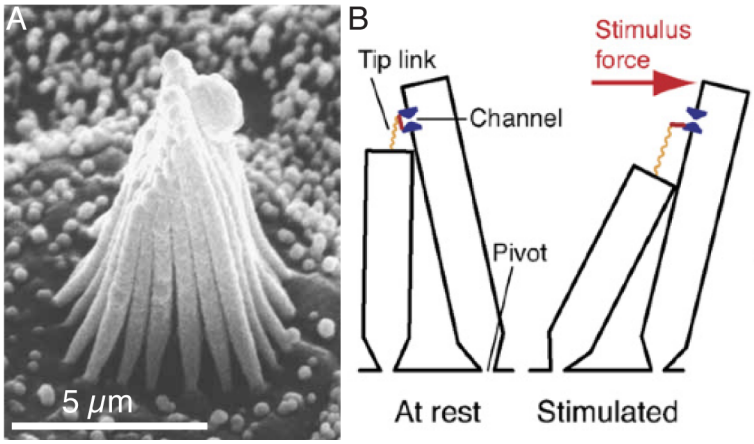

Figure 1.2. Hair-bundle form and transduction. A. Bullfrog cochlear hair bundle with typical height gradation. From Kozlov (2007). **B.** Model of transduction; stereocilia pivot about their tapered bases in response to external forcing, increasing tension in the gating spring, in turn raising the open probability of the transduction channel. Positive or excitatory forces are rightward in this figure. Note this schematic conflicts with data suggesting the channel attaches at the bottom of a tip link (Beurg et al., 2009). Figure adapted from Hudspeth (2008).

With respect to tetrapods, the jawed fishes are the most distant vertebrate relatives whose auditory and vestibular systems have been extensively studied. Their hair cells reside in the inner ear, or labyrinth, where they can detect linear and angular accelerations of the fish's head as well as the near-field component of sounds (Lowenstein and Compton, 1978). In some fishes, coupling of the labyrinth to a gas-filled structure permits the detection of the far-field component (pressure) of sounds (Enger and Andersen, 1967). Other hair cells reside superficially, grouped in neuromasts of the lateral-line system. All the hair bundles of a neuromast project into a common gelatinous encasement termed a cupula, which extends into the water around the fish. As detectors of local fluid

flow (Engelmann et al., 2000), lateral-line hair cells provide fishes with a sense of "distant touch," aiding them in behaviors including schooling and prey capture (Schwarz et al., 2011). The morphology of hair bundles in jawed fish is similar to that of tetrapods: each bundle consists of a single kinocilium at the tallest edge of a beveled array of stereocilia (Popper, 1981) and bears tip links (Söllner et al., 2004). In accordance with their morphological polarization, the hair bundles of jawed fishes are directionally sensitive in their transduction of mechanical stimuli (Obholzer et al., 2008).

The hair cells of jawless fishes, or cyclostomes, reside in organs thought homologous to those described above (Figure 1.3 A). This homology is supported by morphological, developmental, and molecular characters (Hammond and Whitfield, 2006). Nerve recordings suggest that hair cells of the lamprey labyrinth have sensory functions similar to those of jawed fishes; they are sensitive to linear and angular accelerations as well as to vibrations (Lowenstein, 1970). To our knowledge there have been no indications that lampreys or hagfish can detect the far-field component of sound; the apparent absence of air-filled chambers in the cyclostome head seems to obviate the potential for pressure reception (Figure 1.4). Nerve recordings from the labyrinth of the hagfish *Myxine glutinosa* indicate abilities similar to those of lampreys, barring the detection of vibrations (Lowenstein and Thornhill, 1970). Some hair bundles of the hagfish also differ from all other vertebrate hair bundles in their morphology; some bear two kinocilia, others bearing kinocilia positioned in the center of the stereociliary bundle (Lowenstein and Thornhill, 1970) (Figure 1.3 B). This inspires curiosity about transduction in these cells: are they omnidirectionally excitable? This and many similar questions are unexplored; no single-cell recordings of cyclostome hair cells are reported.

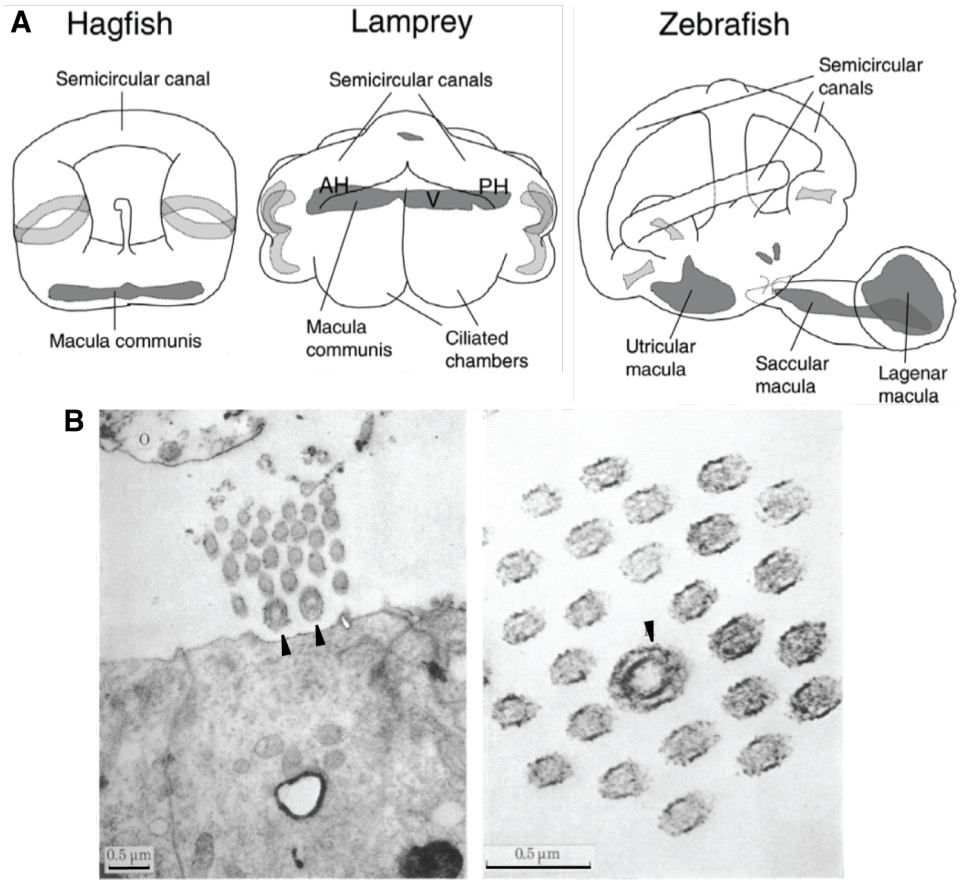

Figure 1.3. The inner ears, or labyrinths, of jawless fish. A. Labyrinth anatomy of representatives of the two clades of jawless fishes - hagfish and lampreys – compared with a teleost fish. Dark gray shading denotes patches of hair cells in sensory maculae, which tend to have dense overlying otolithic structures; light gray denotes patches of hair cells in sensory cristae, which respond to the flow of fluid in the semicircular canals. In hagfish, the macula is not reported to be differentiated into separate structures, as in lampreys and jawed vertebrates. The ciliated chambers are likely unique to the lamprey clade and are of unknown function. AH, anterior horizontal macula, here considered homologous to the utricule of jawed vertebrates, or gnathostomes (Hammond and Whitfield, 2006; Maklad et al., 2014); V, vertical macula, here considered homologous to the gnathostome saccule (Lowenstein et al. 1968); PH, posterior horizontal macula, here considered homologous to the gnathostome lagena (Lowenstein et al. 1968). Figure from Hammond (2006). **B.** Transmission electron micrographs of two hagfish hair bundles. Left, a hagfish hair bundle with two kinocilia (arrowheads). Right, a hair bundle whose kinocilium (arrowhead) is surrounded by stereocilia. Images from Lowenstein (1970).

Figure 1.4. Near-field and far-field sound detection. Blue highlights the first structure to move in response to sound. **A.** The vestibular ear of fishes can detect the near-field component of sound because the entire body moves in response (broken blue line emphasizes the motion of the fish; top, the position of the fish at t = 0 seconds; bottom, the position of the fish at t = 1/2*f* seconds, with *f* = sound frequency in hertz). The motion of the relatively dense otolith (*o*) lags that of the rest of the fish, deflecting hair bundles in contact with the otolith. Adapted from (Fay and Popper, 1999). **B.** Neuromast organs of the fish lateral line consist of hair cells whose kinocilia project into a gelatinous cupula (*c*), which moves in response to water flow, deflecting hair bundles. **C.** The third antennal segment (*a3*) of insects such as *Drosophila melanogaster* can rotate about a flexible joint when the branched arista is vibrated by near-field sound. This rotation deflects processes of sensory neurons housed in scolopidia (*s*) in the second antennal segment (*a2*). Adapted from Boekhoff-Falk (2005). **D.** The far-field component of sound, pressure waves propagating through the surrounding medium, can be detected by fishes whose swim bladder (*b*) is mechanically coupled to the inner ear. The gas in the swim bladder expands and contracts in response to pressure waves; the resulting motion of the swim bladder's wall is propagated to hair cells. **E.** The tympanum of the mammalian ear (blue) vibrates in response to the far-field component of sound due to the oscillating pressure differential between the air on either side. This vibration is transmitted to hair cells in the inner ear through the bones of the middle ear (*h*, *a*, and *s*). From Gray (1918). **F**. Some insects can detect the pressure component of sound. A tympanum (*t*) made of thinned cuticle vibrates, in a manner analogous to that of the mammal tympanum. Tips of scolopidia (*s*) can be directly stimulated by this tympanum.

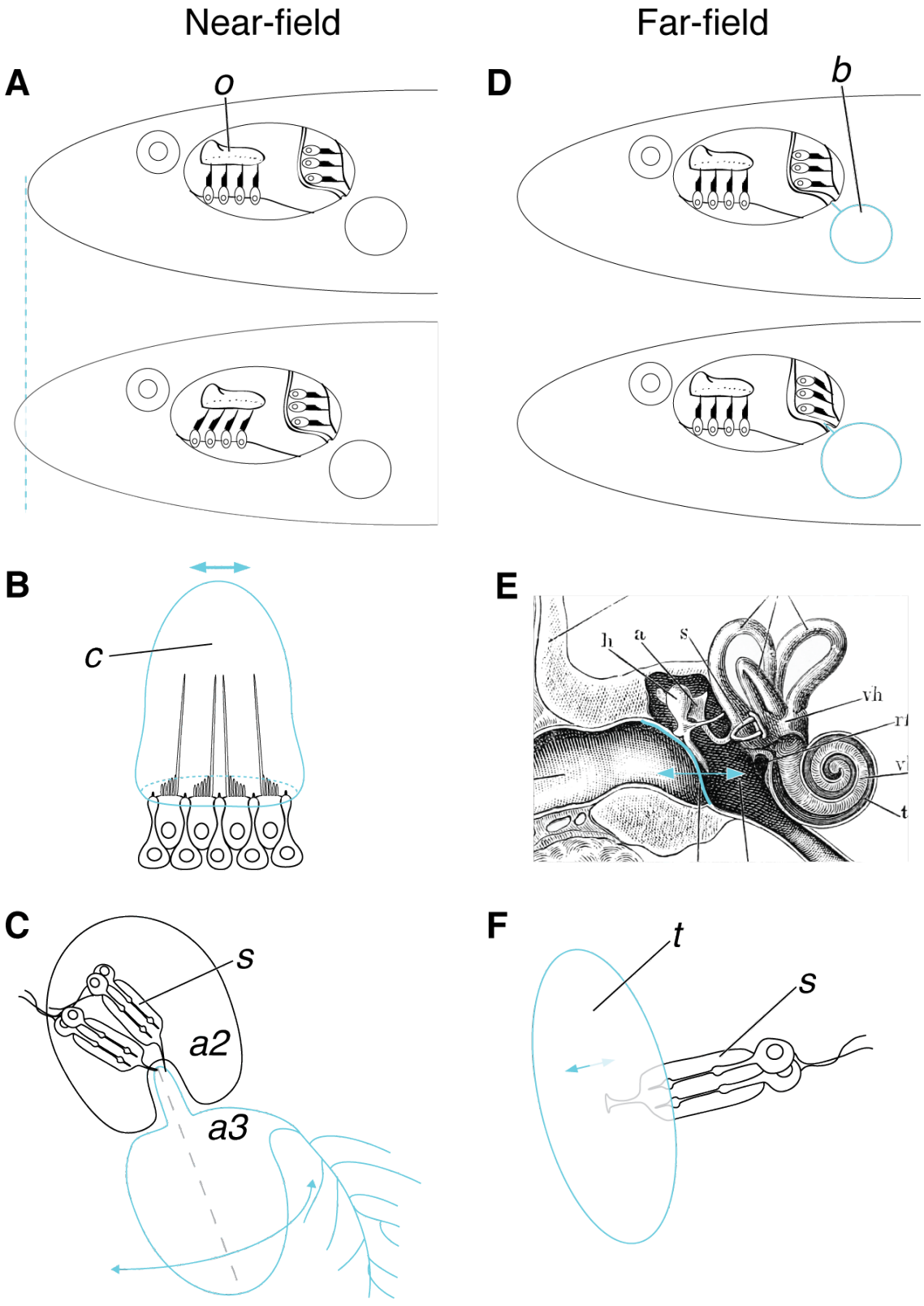

Figure 1.4. Near-field and far-field sound detection

1.2.B. Hair cells in other chordates

Ascidians are marine invertebrate chordates in the clade tunicata, thought to be the sister group to the vertebrates (Ayala et al., 1998). This close alliance is belied by their adult form; ensconced in a tough polysaccharide tunic, adult ascidians live humbly as sessile filter feeders. The interior walls of the incurrent feeding siphon bear a crown of tentacles projecting into the lumen of the siphon (Figure 1.5 A). These tentacles have multiple rows of cells, here called hair cell-like cells (HCLCs) (Figure 1.5 B), with tantalizing structural similarities to vertebrate hair cells: HCLCs have a secondary sensory-cell morphology, with synapses at their basal aspect (Burighel et al., 2003; Caicci et al., 2010). They sport an apical tuft of actin-filled villi which, in a few of the species examined, displays height gradation. Finally, within or at the edge of this bundle are one or two tubulin-filled cilia (Figure 1.5 C). In a baffling twist on the vertebrate theme, some species have a HCLC type whose long kinocilium sprouts from the *shortest* edge of an otherwise monotonically beveled bundle (Manni et al., 2004). This arrangement contrasts with a fundamental concept of hair-bundle function, that deflection toward the tallest edge induces shearing and therefore tenses gating springs - how does one even identify a "tallest edge" in these bundles? Ascidian HCLCs are proposed to be homologous to vertebrate hair cells based on structure, position, and ontogenetic expression of transcription factors (Manni et al., 2004). Although behavioral work indicates that coronal tentacles mediate the rejection of incoming particles (Mackie et al., 2006), no single-cell physiological recordings have been conducted on ascidian HCLCs to confirm their assumed role as mechanoreceptors.

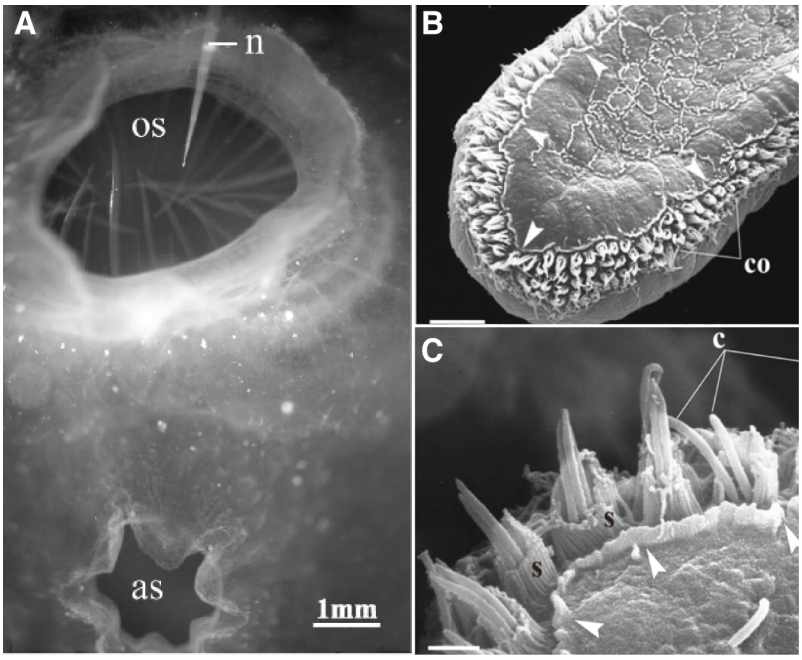

Figure 1.5. The coronal organ of ascidians bears hair-cell-like cells. A. The incurrent oral siphon (os) hosts a ring of tentacles projecting into the incurrent flow, in contrast with the atrial siphon, through which water is ejected. From Mackie (2006). **B.** A scanning electron image of one such tentacle from the ascidian *Molgula socialis*. The coronal organ (co) runs along the tentacle edge. Scale bar 8 μm. **C.** Detail of the tentacle in (B), showing hair-cell-like cells with two kinocilia (c) and a collar of stereocilia (s). Scale bar 1.5 μm. Both scanning electron micrographs from Burighel (2010).

1.3. Active processes in hearing

In the aqueous environment of the inner ear, energy dissipation due to hydrodynamic drag poses a major problem. At this scale, the drag impeding the motion of a structure is proportional to its velocity of motion (Vogel, 1996), painting a particularly grim picture for the detection of high-frequency sounds. Yet animals can be superbly adept at this: echolocating bats and whales have driven their respective targets, some insects and teleosts, to also hear in the ultrasound (Wilson, 2013), and some species of frogs can hear up to 30 kHz (Arch et al., 2009). Hearing high frequencies relies in part on adaptations in passive structures; for example, the tympanal ears of some katydids feature a lever arm, providing a mechanical advantage to combat impedance mismatch at the air-

liquid interface (Montealegre-Z et al., 2012). But in all these groups of animals, the task of hearing also relies on the contribution of mechanically active, energy-consuming amplifiers.

Curiously, auditory amplification occurs in the *same energy modality* as the stimulus; that is, the hearing apparatus mechanically amplifies mechanical signals. Imagine analogs of this feat in other sensory systems: it is fantastic to consider a retina producing photons to brighten an image. Yet the hearing organs of some insects, many tetrapods, and a few bony fishes display evidence of active mechanical amplification, or gain, of their inputs (Ruggero et al., 1997; Martin and Hudspeth, 1999; Nadrowski et al., 2008; Rabbitt et al., 2010). Broadly speaking, among animals three general forms of mechanical amplification have been characterized. In the chordotonal organs of some insects, the auditory receptors perform dynein-based mechanical amplification (Warren et al., 2010; Nadrowski et al., 2008). In a subset of mammalian cochlear hair cells and avian auditory papillar hair cells, proteins called prestin are situated in the basolateral membrane, where it performs mechanical work in response to changes in membrane voltage (Fisher et al., 2012; Beurg et al., 2013). Finally, the auditory and vestibular hair bundles of tetrapod vertebrates display an active process that is driven by myosin motors (Hudspeth and Gillespie, 1994; Le Goff et al., 2005) and is well-described by the general form of a Hopf bifurcation (Hudspeth, 2008). It is this last process, widespread among the tetrapod vertebrates, that this thesis considers.

1.3.A. The hair-bundle active process

The active process of tetrapods, more succinctly referred to as "the active process," harnesses chemical energy to counter the effects of viscous drag in the inner ear. In addition to performing amplification, the active process displays three prominent traits: frequency tuning, compressive nonlinearity, and spontaneous activity. This mechanical amplification is also tuned; a given hair cell's gain can be highest for a specific frequency (Martin and Hudspeth, 1999). Using an array of receptors thus tuned, tetrapod ears can perform a Fourier analysis, decomposing complex sounds into their constituent tones. Furthermore, the active process facilitates the detection of weak sounds; smaller-amplitude stimuli are amplified to a greater degree than are larger stimuli. Through this nonlinear gain, a million-fold range of stimulus amplitudes can drive a mechanical response compressed to a manageable two orders of magnitude (Martin, 2008; Ruggero et al., 1997). Finally, we see that active hair bundles, under specific conditions, can undergo spontaneous oscillations (Crawford and Fettiplace, 1985; Martin and Hudspeth, 1999). This spontaneously oscillating state is considered a by-product, or an epiphenomenon, of the active process; in itself, it does not seem to have sensory utility to an animal. But because spontaneous oscillations stem from the same fundamental mechanisms as does the active process, these unruly movements provide an excellent subject for exploring the basis of mechanical amplification by tetrapod hair bundles. Below we will outline how the interaction of two hair-bundle processes, transduction and adaptation, can together give rise to spontaneous oscillations. We will then consider the relationship between spontaneous oscillations and the amplifying abilities of the active process.

1.3.B. Transduction generates negative stiffness

We earlier described that hair bundles can directly transduce mechanical stimuli, allowing very rapid responses. Direct transduction gives rise to another important feature of hair bundles: nonlinear stiffness. In its most striking form, this nonlinearity is so strong that the bundle displays a region of negative stiffness. Negative stiffness defies intuition derived from everyday physics; if one pushes a negatively stiff object, the object does more than comply: it *pulls* the pusher along! This behavior is sometimes exhibited by hair bundles. Displacement-force relations of frog saccular hair bundles (Martin et al., 2000) display a region of negative slope, or negative stiffness (Figure 1.6). Turtle cochlear bundles also display nonlinearity; however, the kink in their stiffness profile has been shown to have a greatly reduced, but not quite negative, slope (Ricci et al., 2002). Most objects follow Hooke's law for such modest deformations, so this unusual behavior begs an explanation. Negative bundle stiffness emerges from transduction mechanics; because channel gates and gating springs affect one another reciprocally, a bundle's channels gate with positive cooperativity. That is, one channel's opening increases the probability that the other channels will open. Thus, the bundle will not reside stably – it is negatively stiff – through the range of deflections over which gating occurs.

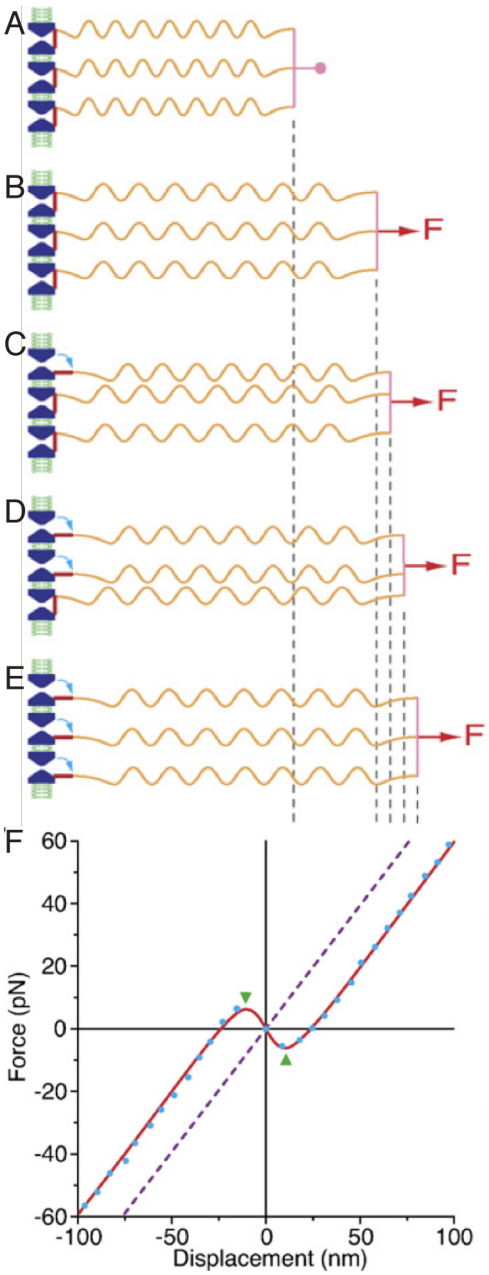

Figure 1.6. Gating of hair-cell transduction channels generates negative stiffness. A. Three mechanotransduction channels (blue) gating in parallel with one another are, for simplicity, drawn in the same membrane. Each channel is in series with its own elastic gating element, fixed to an adjacent stereocilium (pink line). These three gating springs are initially relaxed. **B.** A constant force F is applied, stretching all three gating springs. Increased tension in each of the springs elevates the probability that the associated channel will open. **C.** One channel yields first, and opens. The swing of the channel gate (red) relieves the associated spring of some extension, so it relinquishes some of its load-bearing duties; under the constant force, the motion of the stereocilia increases further (emphasized by dotted lines). The other two gating springs thus suffer a further increase in tension, increasing their associated channels' open probabilities even more. **D.** Another channel opens, allowing its gating spring, too, to shorten. The stereociliary movement increases even more. **E.** This burdens the last gating spring with even greater tension, assuring a very high probability of the last channel quickly opening. Thus the concerted, parallel gating of transduction channels can make a group of gating springs appear more compliant to a constant force. **F.** Using a flexible fiber, one can hold a hair bundle at displacements along its axis of sensitivity while recording the force exerted by the fiber at each displacement. In force-displacement relations of healthy bullfrog hair bundles, there is a region of negative slope, or negative apparent stiffness. This corresponds to the range of displacements over which transduction gating occurs. Figure from Hudspeth (2008).

1.3.C. Myosin motors power adaptation

A sufficient displacement in the positive direction snaps open all the transduction channels, generating a saturated receptor current. In the face of sustained stimuli, such as gravitational forces conveyed by overlying structures, this saturation could overwhelm the bundle, preventing faithful transduction of small oscillatory stimuli. As an apparent solution, hair cells, like most other sensory cells, are able to adapt. Their hair bundles orchestrate mechanical rearrangements to adjust the relationship between bundle displacement and channel open probability (P_o). Adaptation occurs in fast and slow phases whose underlying mechanisms seem functionally distinct. Fast adaptation causes the receptor current to decay exponentially with a time constant of several milliseconds or less. Although investigators agree that fast adaptation stems from negative feedback on channel P_o by the Ca^{2+} component of the transduction current, the specific feedback mechanism is unresolved (Benser et al., 1996; Cheung and Corey, 2006; Bozovic and Hudspeth, 2003). In the slow-adaptive phase, the receptor current exponentially decays from its initial response with a time constant of roughly 30 ms. Simultaneous monitoring of the bundle's motion reveals a mechanical correlate at the same timescale: after the onset of a force step, the bundle relaxes further in the direction of the stimulus. It was proposed that molecular motors move along stereociliary actin to adjust gating spring tension, and thus adjust the range of bundle deflections over which channels gate (Figure 1.7) (Holt et al., 2002; Hudspeth and Gillespie, 1994).

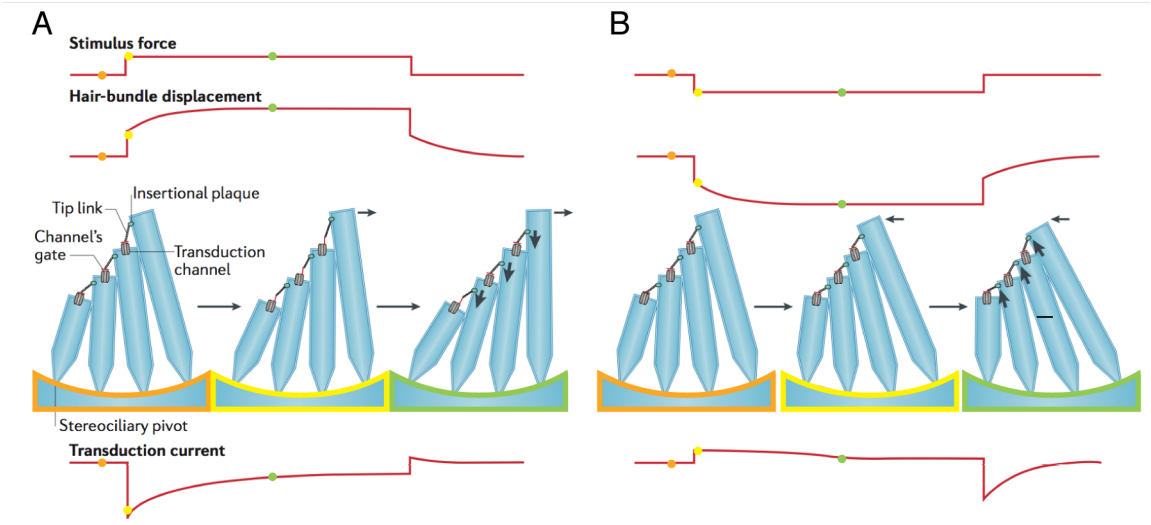

Figure 1.7. Adaptation in hair cells. This figure depicts hair-bundle displacement and transduction current in response to forces along the bundle's axis of sensitivity. Also shown are schematized snapshots in time of the hair bundle's transduction complex. **A.** Before the application of an external force (orange), the hair bundle's displacement is steady. Most of the transduction channels are closed at rest, yielding only a small inward current. A force toward the bundle's taller edge first causes the bundle to abruptly jump forward (yellow), tensing the gating springs (shown here as tip links), opening transduction channels, and allowing a large inward current. Ca^{2+} carried by this inward current influences the adaptation motor, causing the insertional plaque to slip downward (black downward arrows). As a result, the hair bundle slowly relaxes farther in the direction of the stimulus (green); concomitant with this, the channels reclose, accounting for the declining inward current. **B.** When forced toward its shorter edge, a hair bundle initially jumps in that direction (yellow), which slackens the gating springs beyond their resting state and reduces the inward current to zero. This eliminates a source of Ca^{2+} entry into the stereocilia, allowing adaptation motors to climb (black upward arrows) and increase the tension in tip links, which slowly draws the hair bundle farther in the direction of the stimulus (green). This accounts for a reopening of channels, allowing the inward current to approach its resting level. Figure slightly adapted from Hudspeth (2014).

Myosin Ic is presumed to serve as the adaptation motor in nonmammalian tetrapods; its transcript is found in bullfrog hair bundles (Metcalf et al. 1994) and the protein can be immunolocalized at stereociliary tips, the site of mechanoelectrical transduction (García et al. 1998). The number of myosin Ic molecules estimated by that structural study, as well as by biochemical studies (Gillespie et al. 1993, Walker et al. 1996) agree with predictions of motor number based on observed hair-cell physiology (Gillespie and Cyr, 2004). By introducing a single point mutation in myosin Ic that confers susceptibility to inhibition by an ADP analog, Holt and colleagues (2002) showed that myosin Ic is a necessary adaptation motor in mouse hair bundles.

To perform adaptation, a motor should have some way of relating its activity to the state of the transduction apparatus. There is a wealth of evidence that the Ca^{2+} component of the transduction current feeds back on the rate of adaptation (Hudspeth and Gillespie, 1994; Walker and Hudspeth, 1996; Martin et al., 2003; Manley et al., 2004; Ricci et al., 2002), but the exact mechanism by which Ca^{2+} alters the climbing and slipping rates of myosin Ic is debated (Gillespie and Cyr, 2004).

1.3.D. Negative stiffness and adaptation yield spontaneous oscillations

Under certain conditions, hair bundles can spontaneously undergo low-frequency, large-amplitude, periodic movements (Figure 1.8 A). The canonical waveform of spontaneous oscillations – slow movements interspersed with catastrophic leaps – is suggestive of a "relaxation oscillation." This term is used to describe a wide range of processes, from temperature fluctuations in a thermostat-controlled home to chalk squeaking on a blackboard (Pippard, 2007 p. 42). Uniting these examples is that some variable in the system (*e.g.,* air temperature) is actively driven toward a steady state (*e.g.,*

by fuel combustion), but before this state is reached, the system crosses an instability (*e.g.,* the temperature hits the thermostat's set point), triggering an abrupt change in the system's behavior. With this analogy in mind, it is attractive to consider that spontaneous hair-bundle oscillations are powered by the work of myosin motors striving to bring gating-spring tension to a steady state, at some point triggering the all-or-nothing gating of transduction channels. Indeed, by measuring the displacement-force relations at different points in a hair bundle's spontaneous oscillations, we see that these oscillations emerge when slow adaptation vainly attempts to place the bundle where it cannot stably reside: in its region of negative stiffness (Figure 1.8 B) (Le Goff et al., 2005). This model is also supported by ionic and pharmacological perturbations of spontaneously oscillating bullfrog hair cells. High concentrations of external Ca^{2+} can halt spontaneous oscillations (Martin et al., 2003) by biasing the hair bundle toward its shorter edge, consistent with this cation inhibiting the adaptation motor's force production. Furthermore, pharmacological blockade of myosins can reversibly freeze oscillations (Martin et al., 2003). The mechanical instability wrought by channel gating is also apparently necessary for spontaneous oscillations. An aminoglycoside antibiotic, gentamicin, can blunt the inward currents normally evoked by deflection of hair bundles, indicating that this drug blocks conductance through transduction channels (Kroese et al. 1989) by locking them in their "open" configuration. Gentamicin was also shown to remove the kink in the displacement-force relation of bullfrog hair cells (Howard and Hudspeth, 1988). In the original description of amphibian hair-bundle spontaneous oscillations, these movements were reversibly inhibited by gentamicin (Martin et al. 2003).

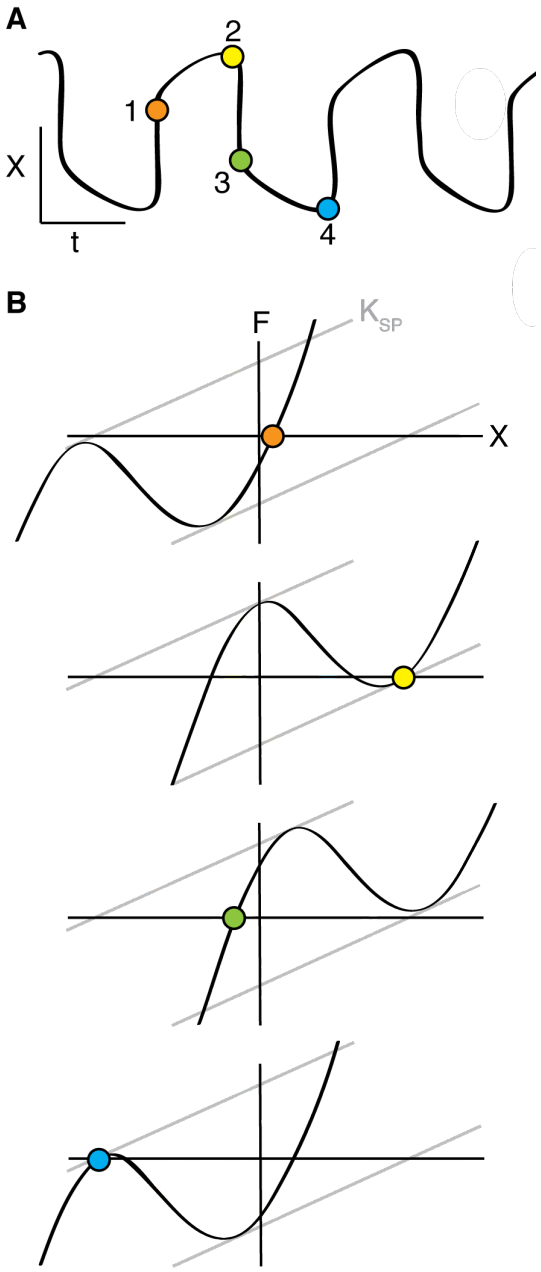

Figure 1.8. Spontaneous hair-bundle oscillations emerge from negative stiffness and slow adaptation. A. The motion X of a spontaneously oscillating hair bundle over time (t) often shows two timescales: slow relaxations (1 → 2 and 3 → 4) interrupted by abrupt jumps (2 → 3). **B.** Theoretical displacement-force relations of a hair bundle. This bundle's stiffness curve has a region of negative slope. We consider here a situation in which bundle motion is spontaneous; that is, with no application of external force. The bundle's state (colored dot) is therefore constrained to the horizontal axis. Four curves, successive snapshots in time corresponding to the points in (A), show that myosin-based adaptation slowly shifts displacement-force curves along the line whose slope is set by the stiffness K_{SP} of the stereociliary pivots. The bundle initially lies to the right of its nonlinear region (orange), indicating that nearly all transduction channels are open. Responding to Ca^{2+} influx through open channels, myosin Ic slips, relieving gating-spring tension, and brings the bundle closer to its nonlinear region (yellow). When myosins slip enough to bring the bundle into its region of negative slope, in which channels cooperatively slam shut, the bundle jumps to a much more negative position (green). Without the Ca^{2+} influx through open channels, myosin Ic is free to climb, building tension in the gating springs, until the channels are just on the cusp of cooperatively snapping open (blue). Figure drawn from Martin (2000).

1.3.E. Spontaneous oscillations

If we grant that ears are for listening to the outside world, what is the relevance of spontaneous oscillations? It is clear that a hair bundle undergoing these unprompted movements can be coaxed into usefulness: when stimulated with a sinusoidally driven flexible fiber, the bundle entrains its motion to the stimulus (Martin and Hudspeth, 1999); in so doing, its amplitude can exceed, and its phase can lead, that of the fiber. This amplification is not uniformly applied to all stimuli, but is most prominent at specific frequencies and for small stimuli. These interrelated traits – amplification, frequency tuning, compressive nonlinearity, and spontaneous oscillations – are all indicative of a system operating near a dynamical instability termed a Hopf bifurcation (Strogatz, 1994; Martin, 2008). This categorization, rather than pinpointing the exact mechanism of the hair-bundle active process, is useful in describing its behavior. Viewing the active process as governed by Hopf dynamics helps us predict, for instance, how inter-taxonomic differences in hair-bundle stiffness might impinge on their amplifying abilities.

1.4 Evolution of the hair bundle's active process

Hair bundles are far from passive receivers of mechanical stimuli, but are instead active participants in the processes of transduction. This understanding draws from findings in the tetrapod clade, including frogs, turtles, lizards, birds, and mammals. But is this trait unique to the tetrapods, or did it evolve before the emergence of this clade (Figure 1.9)? We have a burgeoning understanding of hair-cell physiology in the jawed fishes, revealing some intriguing evidence for an active mechanical process in their hearing organs. Imaging cupulae in the semicircular canals of the oyster toadfish,

Opsanus tau, reveals one hallmark of the active process, termed compressive nonlinearity, wherein small-amplitude stimuli elicit greater gain than do large-amplitude stimuli (Rabbitt et al., 2010). A similar study of the African knifefish, *Xenomystus nigri,* lateral line indicates nonlinear cupular mechanics (van Netten and Khanna, 1994). Finally, a study of inner-ear hair cells in eels revealed spontaneous and electrically evoked kinociliary movements, but it is unclear whether these motions are related to the myosin-based active process of tetrapod hair cells (Rüsch and Thurm, 1990).

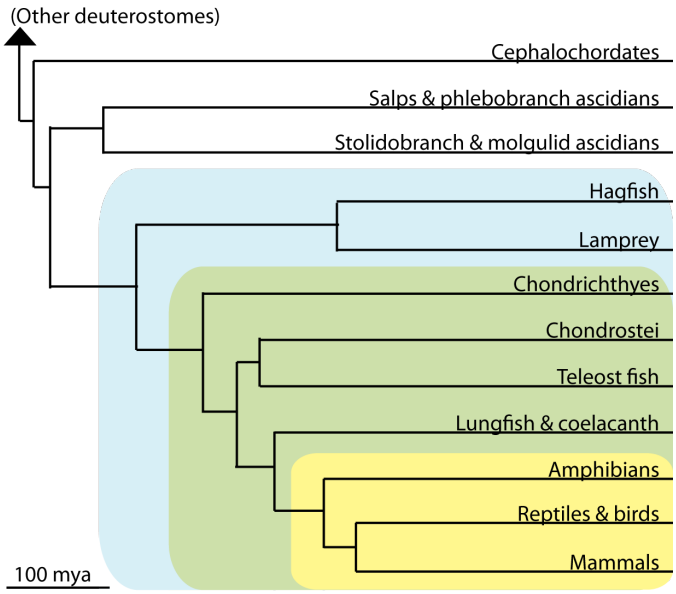

Figure 1.9. The interrelationships of major chordate groups. Blue circumscribes all vertebrates, including the jawless fishes and their most recent ancestor in common with jawed vertebrates. Green highlights all jawed vertebrates, also termed gnathostomes. Yellow highlights the tetrapods. Divergence times of sister groups drawn here come from fossil evidence summarized by Blair (2005), representing a minimum boundary. The split between jawless/jawed vertebrates is accordingly drawn at 520 million years ago (Shu, 1999), but could be as ancient as 650 million years ago according to a Baysian analysis of amino acid divergence (Blair and Hedges, 2005).

In contrast, from jawless vertebrates and ascidians come no reports on the physiological properties of single hair cells. This gap in our knowledge makes it very difficult to consider the evolution of the hair-bundle active process in chordates. As a first

step in exploring the evolution of mechanical amplification, we characterized the mechanical behaviors of hair bundles from the inner ears of two jawless vertebrates, the sea lamprey *Petromyzon marinus* and the American brook lamprey *Lampetra appendix*. To our surprise, we observed robust spontaneous hair-bundle oscillations in both of these animals. To address whether these movements are homologous to those seen in tetrapod vertebrates, we studied the mechanisms driving spontaneous oscillations in *L. appendix*. One set of experiments suggested that Ca^{2+} serves as a signal by which the state of transdution channels can feed back on the activity of adaptation motors, a finding consistent with the oscillation mechanism known from tetrapods. Application of gentamicin, a drug known to block hair-cell transduction channels in tetrapods, reversibly halted spontaneous oscillations in *L. appendix*, suggesting their channels, too, are sensitive to this drug. Furthermore, we found spontaneous oscillations in the *L. appendix* ear to be sensitive to a broad-spectrum myosin inhibitor called butanedione monoxime, a result mirroring that seen in tetrapod hair bundles. To more precisely probe the mechanistic underpinnings of *L. appendix* spontaneous oscillations, we employed pentachloropsuedilin, an inhibitor specific to class-I myosins. These experiments, in contrast to all the others, suggested a possible difference between bullfrog and lamprey spontaneous oscillations. Finally, we demonstrated that *L. appendix* hair bundles exhibiting these movements can entrain to and mechanically amplify particular stimulus frequencies.

2. Materials and methods

2.1. Ca^{2+}-sensitive microelectrode recordings

We made Ca^{2+}-sensitive microelectrodes from double-barreled theta glass (Warner Instrument Corp.). We pulled the glass on a coil-filament, solenoid-assisted vertical pipette puller, yielding electrodes with a taper length of approximately 25 mm. At the unpulled end of the electrode, we chipped away 5 mm of one barrel's rounded wall; this would aid in later differentiating the reference from the ion-sensitive barrel and in providing electrical insulation between the two. We then broke the tip of the electrode against a glass slide to an outer diameter of 5 μm. We filled the Ca^{2+}-sensitive barrel with 150 mM $CaCl_2$ and the reference barrel with 150 mM NaCl, each filtered through a 0.22 μm syringe filter (Millipore). To prevent formation of salt bridges between the two barrels, we passed the unpulled end of the electrode through a flame. We inserted a Teflon tube in the Ca^{2+}-sensitive barrel and a Ag/AgCl electrode in the other, and sealed both in with melted dental wax. The Teflon tube served as an adaptor for a plastic syringe.

We prepared a solution for silanizing the Ca^{2+}-sensitive barrel: 4% (by volume) trimethylchlorosilane (Sigma) in xylene. All steps performed with silane took place in a fume hood. Mounted on a manipulator and under microscopic guidance (30 X total magnification), the electrode was lowered into the silane solution. Using the syringe, we pressure-ejected a small bubble of $CaCl_2$ solution. We drew in the silane solution to a height of roughly 2 mm, then repeated the steps of ejection and filling several times. After a final ejection of the silane solution, we maintained positive pressure on the pipette and moved the electrode to a vial of calcium ionophore I, cocktail A (Sigma) in xylene, at

which point the syringe was removed and the barrel allowed to equilibrate to ambient pressure, drawing some ionophore into its tip. This created a liquid "membrane" with selective permeability to Ca^{2+} mediated by the ionophore. We then threaded an Ag/AgCl wire through the Teflon tubing and sealed this with dental wax. We calibrated the electrodes in a series of solutions ranging in two-fold steps from 10 μM to 160 μM Ca^{2+}, with an additional solution of 1.3 mM Ca^{2+}. All these solutions contained either 150 mM NaCl or KCl. Initially we employed NaCl as this background salt, but we changed this to KCl in accord with an assumption that some compartments in the lamprey ear are endolymph-like with K^+ as the dominant cation. If an electrode displayed no Ca^{2+} sensitivity or a sub-Nernstian slope, we could sometimes salvage the electrode by again flaming its blunt end.

We then decapitated a lamprey and pinned its head ventral side up in a Sylgard-coated dish in ice-cold perilymph solution. We split the head laterally along the midline. One half of the head went immediately into a 4 °C refrigerator for later use. The other half we dissected and pinned with the medial face of the otic capsule directed upward. We ensured the ear was higher than the rest of the tissue, permitting us to wick saline solution away from the point of microelectrode entry without flooding the ear with the artificial saline solution. We placed a pelleted Ag/AgCl ground electrode in this saline solution bathing the ear. We then positioned the Ca^{2+}-sensitive microelectrode in the ear and continuously monitored the voltage in both microelectrode barrels with a chart recorder. When steady voltages were achieved for roughly a minute, we used those

values to calculate the voltage and the extracellular Ca^{2+} concentration *C* (Nicholson, 1993):

$$C = (C_0 + K) \bullet 10^{\frac{V - V_0}{M}} - K; \quad (1)$$

with *M* the slope of the Ca^{2+}-sensitive barrel, *V* the voltage of the Ca^{2+}-sensitive barrel minus the voltage of the indifferent barrel, C_0 a reference Ca^{2+} concentration, V_0 the voltage of the Ca^{2+}-sensitive barrel minus the voltage of the indifferent barrel in that reference solution, and *K* the calculated interference from background ions.

After noting a compartment of interest, we performed an experiment to label this site. The indifferent barrel of the electrode was filled with 150 mM NaCl as usual, but the second barrel was filled with 50 mg/mL Alcian blue (Electron Microscopy Sciences) in 150 mM NaCl. When the signal from the indifferent barrel indicated that it had reached the site of interest, we pressure-ejected the dye. The ear was then fixed in 4% formaldehyde in perilymph solution overnight, rinsed in normal perilymph solution, dissected from its cartilaginous capsule, and visualized.

2.2. Physiological saline solutions

We prepared all saline solutions as Ca^{2+}-free 10X stocks that were stored in frozen aliquots. After thawing an aliquot and diluting it to working concentration, we oxygenated the solution on ice, added $CaCl_2$, and ensured its pH was 7.2 – 7.3. Lamprey perilymph solution contained 109 mM Na^+, 2.1 mM K^+, 1.8 mM Mg^{2+}, 1 mM Ca^{2+}, 116 mM Cl^-, 4 mM D-glucose, and 2 mM HEPES. Bullfrog perilymph solution contained 114 mM Na^+, 2 mM K^+, 2 mM Ca^{2+}, 118 mM Cl^-, 5 mM HEPES, and 3 mM D-glucose. For both species' perilymph solutions we made pH adjustments with HCl or NaOH.

Lamprey and bullfrog endolymph solutions contained 117.5 mM K^+, 2 mM Na^+, 118 mM Cl^+, 3 mM D-glucose, and 5 mM HEPES; we made pH adjustments with HCl or KOH. The concentration of Ca^{2+} in lamprey endolymph solution differed between experiments; when Ca^{2+} was iontophoretically controlled, the endolymph solution contained baseline concentration of 40 μM Ca^{2+}. For all other studies of lamprey spontaneous oscillations the endolymph solution contained 50 μM Ca^{2+}. In experiments with bullfrog hair cells the concentration of Ca^{2+} in the endolymph solution was 250 μM.

2.3. Dissecting the lamprey ear

We procured lamprey larvae of both species, *Lampetra appendix* and *Petromyon marinus*, which were caught from streams in the lower peninsula of Michigan by Lamprey Services (Ludington, MI). We housed the lampreys according to animal protocol number 13605 of The Rockefeller University IACUC in species-specific, aerated aquaria at 4 °C . These aquaria were lined with several inches of sand to satisfy one of the strongest behavioral preferences of these animals, burrowing (Francis and Horton, 1936). We netted lampreys to be used for an experiment and transported them in a smaller container of ice water, which was also lined with sand.

We decapitated a lamprey with a scalpel just anterior to third gill opening and pinned the head ventral side up in lamprey perilymph solution. With coarse iridectomy scissors, we cut along the ventral midline. We pinned out the ventral body wall so that the pharynx and cranial cavity were visible. Being careful not to damage the otic capsules, we cut through the cartilaginous brain-case with coarse iridectomy scissors to destroy the brain.

All solutions were kept on ice unless otherwise noted. We removed both otic capsules from the head, keeping a significant length of anterior brain-case cartilage attached to each capsule. Because the ears are otherwise nearly symmetrical about the anteroposterior axis, this aids in distinguishing left from right ears. With fine iridectomy scissors, we gently nicked the membrane covering the medial window into the ear, providing a pressure outlet to prevent later damage to the ear. Using coarse iridectomy scissors, we removed a small area of the cartilaginous capsule on the dorsal aspect, allowing visualization of the anterior and posterior semicircular canals and ciliated chambers. Using fine iridectomy scissors, we cut open the semicircular canals and ciliated chambers.

We then bathed the ears in 50 μg/mL protease XXIV (Sigma) in lamprey perilymph solution and rotated the otic capsules so the windowed area of their dorsal aspect faced down. We balanced on a dissection pin the brain-case cartilage projecting from the anterior end of the ear, elevating the anterior portion of the ear. This orientation promoted detachment of the large utricular otolith during the protease incubation. We allowed the incubation to proceed at room temperature for five minutes or until we could visually confirm the loosening of the utricular otolith.

After returning both otic capsules to regular lamprey perilymph, we stored one ear, to be used later, in this solution on ice. The other ear we removed from the outer cartilaginous capsule and pinned down at its posterior half with its dorsal side facing up. Using fine iridectomy scissors, we removed the ciliated chambers and semicircular canals, then trimmed the margins of the utricle.

We next mounted the utricle in a two-chamber apparatus, allowing the hair cells' apices to project into endolymph solution while their basolateral surfaces were bathed in perilymph solution. We first fashioned discs onto which the utricle would be glued. These were made from 7 μm-thick polymer shrink-wrapping into which a hole of 200-μm diameter was cut with a CO_2 laser. Using a glass pipette with its tip broken to easily accommodate the utricle, we transferred this tissue to the top of a disc and positioned it, apical side down, over the disc's hole. With a corner of a Kimwipe we carefully removed fluid from the basolateral side of the utricle. Using a Teflon spatula, we then applied n-butyl cyanoacrylate glue (Vetbond, 3M) to the margins of the epithelium, aiming for a complete seal without allowing the glue to creep over the epithelium. Finally, we transferred the disc, apical side up, to a two-chamber apparatus with perilymph solution in the bottom compartment and endolymph solution in the top compartment.

2.4. Recording the motion of hair bundles

We observed the utricular epithelium with an upright microscope (Olympus BX51WI) equipped with differential-interference-contrast optics and a 60X water-immersion objective lens (LUMPlan FL N, ∞/0/FN26.5). For viewing hair bundles by eye, we illuminated the preparation by white light (Olympus TH4-100). For making high-resolution recordings of the motion of hair bundles, we illuminated the preparation with a red light-emitting diode (Prizmatix ultra high-power LED, Givat-Shmuel, Israel). The light followed a path yielding an optical gain of 1500 before reaching the dual-photodiode circuit (Sanjee Abeytunge) whose output signal was linearly related to the displacement of a shadow along its sensitive axis. This output signal was low-pass filtered at 2 kHz (Kemo BM8) before being digitally converted (National Instruments

BNC-2090A) at 100 μs intervals. We translated this signal into the magnitude of hair-bundle displacement by calibrating the sensitivity of the photodiode: between successive recordings we displaced the shadow a known amount with a mirror mounted on a closed-loop piezoelectric actuator (Piezosystem Jena 87959). For recording the motion of free hair bundles, we lowered the condenser lens to maximize optical contrast of the hair bundle's shadow at the level of the photodiode. For recording the motion of hair bundles that were attached to a flexible force-fiber, the fiber provided the shadow whose motion was recorded.

2.5. Iontophoresing Ca^{2+} and gentamicin

To observe the response of lamprey hair bundles to Ca^{2+}, we controlled the concentration of this ion in the vicinity of a hair bundle using iontophoresis from a pipette. As the migration of ions in a voltage gradient, this process would ideally be controlled by the Hittorf equation (Purves, 1981):

$$q = \frac{-n \bullet I}{z \bullet F} \tag{2}$$

where q is the efflux of the ion, in this case Ca^{2+}, and n is the transference number 0.12 (Tinevez et al., 2007), I is the current, z is the charge number of the ion, and F is Faraday's constant. However, at least two other processes can affect the discharge of ions from a iontophoretic pipette. The first of these processes is the diffusive release of the ion, which can be approximated by (Purves, 1981):

$$q_D = \pi \bullet D \bullet C_0 \bullet \theta \bullet a \tag{3}$$

with D the diffusion coefficient of the ion in water, a the internal radius of the pipette tip, 2θ the pipette tip's included angle, C_0 the initial concentration of the ion inside the pipette tip, and q_D the steady-state diffusive release of the ion. Another process affecting the release of an ion from the pipette is bulk flow, driven by gravity; the release attributable to this is governed by (Purves, 1981):

$$q_H = \frac{3\pi \bullet \theta \bullet \rho \bullet g \bullet h \bullet C_0 \bullet a^3}{8\eta} \tag{4}$$

in which g is the gravitational attraction, ϱ the density and η the viscosity of the filling solution, and h the height of the liquid column. To determine the range of ejection currents we would apply, we considered that the steady-state concentration of an ion x at a given distance r from the iontophoretic pipette can be approximated by (Tinevez et al., 2007):

$$x(r) = x_0 + \frac{n \bullet I}{4\pi \bullet D \bullet z \bullet F \bullet r} \tag{5}$$

in which x_0 is the concentration of the ion in the extracellular medium before the onset of iontophoresis.

Because the processes governed by equations (3) and (4) are independent of the ejection current I, at low values of I the relationship between q and I is markedly nonlinear. This was problematic, for we wanted to precisely command relatively small changes in Ca^{2+} concentration. To overcome this, we attempted to achieve the set of conditions allowing the iontophoretic release q to dominate over q_D and q_H. This effort was aided by the similar dependency of q_D and q_H on C_0, a, and θ. Reducing the values of

these three parameters should decrease the nonlinearity in the *I-q* relationship. Lower values for these three parameters also increase the electrical resistance of a pipette; pipette resistance therefore served as our proxy for estimating how linearly a pipette would behave when commanded to iontophorese miniscule doses of Ca^{2+}.

Purves (1979) analyzed this exact problem and determined that iontophoretic ejection voltages exceeding 100 mV position the system at an approximately linear region of the *I-q* relationship. Knowing this minimum ejection voltage (V_{min}) and the resistance of the iontophoresis pipette ($R_{pipette}$), we calculated the minimum ejection current ($I_{\min}$) :

$$I_{\min} = \frac{V_{\min}}{R_{pipette}} \tag{6}$$

using the value of I_{min}, our desired minimum increase in Ca^{2+} concentration ($\Delta Ca^{2+}{}_{min}$), and equation (4), we calculated r with the following relation, with SI units for all variables:

$$r = \frac{0.52 \bullet n \bullet I_{\min}}{\Delta Ca^{2+}{}_{\min}} \tag{7}$$

With desired $\Delta Ca^{2+}{}_{min}$ values ranging from 10 μM to 50 μM, and a range of 1 μm to 10 μm considered practical for r, ideal values for $R_{pipette}$ were bounded by 25 and 100 MΩ. We found that pipettes whose $R_{pipette}$ values exceed 80 MΩ are susceptible to clogging.

We filled iontophoresis pipettes with 120 mM $CaCl_2$. Using this filling solution, we tested the $R_{pipette}$ values of pipettes pulled on a Sutter P-80 programmable pipette

puller from 1.2 mm outer diameter borosilicate glass (WPI, 1B120F-3). We empirically determined a program that consistently delivered an appropriate range of $R_{pipette}$ values.

During an experiment, we positioned the iontophoretic pipette at the distance *r* from a lamprey hair bundle. For baseline recordings, we applied a negative current of -4 nA to restrict diffusive release of Ca^{2+}. All commands sent to the iontophoresis electrode were generated in LabView and delivered by an Axoclamp 2B amplifier (Axon Instruments) in bridge mode.

To iontophorese controlled amounts of gentamicin, we used the same protocol for pipette fabrication. The pipette filling solution was 120 mM gentamicin sulfate with 20 mM KCl added to prevent electrode polarization. We then lowered the pH of this filling solution below 5 to promote protonation of gentamicin's amino groups, thus promoting the molecule's iontophoretic ejection. When filled with this solution, the pipettes had an electrical resistance of 10 – 100 MΩ. When not intending to eject gentamicin, we retained the drug in the pipette using a holding current of – 2 nA. In calculating the gentamicin concentration evoked by a given iontophoretic current, we assumed the ratio of gentamicin's transference number to its valence was 0.013 (Jaramillo and Hudspeth, 1991).

2.6. Mechanically stimulating hair bundles

We fabricated flexible stimulus fibers from the same borosilicate glass used to manufacture iontophoresis pipettes. We introduced an initial taper to each fiber with an electrode puller, melted this tapered end onto a heated platinum filament, and used a solenoid to pull a glass wisp perpendicular to the long axis of the taper. This procedure yielded a glass wisp of about 1 μm diameter cantilevered out from the glass shaft. To

enhance the optical contrast of this thin fiber, we coated each stimulus fiber with a layer of gold-palladium (Hummer 6.2, Anatech). We aimed to achieve fibers with stiffnesses K_{SF} of 50 – 300 $\mu N \cdot m^{-1}$ and hydrodynamic drag coefficients ξ_{SF} of 40 – 300 $nN \cdot s \cdot m^{-1}$. We calculated these values by fitting to a Lorentzian relation the power spectrum of each probe's Brownian motion in water (Benser et al., 1996; Howard and Hudspeth, 1988).

To facilitate adherence of the stimulus fiber to the kinocilium of a lamprey hair bundle, we immersed the tip of the fiber in a solution of 1 mg/mL concanavalin A (Sigma) in water for ten minutes. We allowed the fiber to air-dry for several minutes before introducing it into the endolymph solution in the experimental chamber. The fiber was mounted to the end of a piezoelectric actuator (Piezosystem Jena, 94182). We sent displacement commands of magnitude Δ to this actuator, resulting in a displacement of the base of the fiber by that same magnitude. We generated the commands in LabView and produced an analog signal with a National Instruments board (BNC-2090A). We made a thermal insulation sleeve for this piezoelectric actuator to limit low-frequency drift.

2.7. Analyzing spontaneous oscillations

All data analysis was performed in Matlab. To analyze the spontaneous oscillations of a lamprey's hair bundle, we calculated various metrics of the oscillation waveform. For oscillations whose fast and slow timescales of motion were sufficiently distinct, we were able to calculate the positive and negative residence times. These values describe the average duration an oscillating hair bundle spent residing in the slowly relaxing states punctuated by abrupt lurches. We employed a jump-detecting algorithm to calculate these residence times. We smoothed the displacement data $X(t)$ with a

rectangular moving average whose duration was equal to one-tenth the period of oscillation, as determined by a local peak in the power spectrum of hair-bundle motion. We then calculated dX/dt and smoothed these data with another rectangular moving average. When dX/dt remained above or below empirically determined thresholds for a empirically determined duration, the algorithm declared a positive or negative jump, respectively. A stretch of data preceded by a positive-going jump and followed by a negative-going jump was considered a positive residence event, and its duration was recorded. We followed this same logic to calculate negative residence times. If the oscillation was particularly irregular, our algorithm occasionally reported jumps of the same polarity adjacent to one another; we discarded the intervening data. For a set of recordings whose residence times were to be compared, we employed the same empirically determined analysis parameters.

When an oscillation was too irregular to be reliably analyzed by the above procedure, we employed a different algorithm to analyze the relative times spent in the positive and negative states. We first used a rectangular moving average with a duration of several seconds to calculate the slow drift on which the spontaneous oscillations were superimposed. After eliminating this slow drift, we quantified the fraction of time that X was found to be greater than the median value of X.

Hair bundles of the bullfrog's sacculus sometimes undergo multimodal oscillations, characterized by periods of oscillatory bursting interspersed with slow relaxations. We wrote an algorithm to calculate the average duration spent in these two states. Over a sliding bin of empirically determined width, the standard deviation of X

was measured. When the standard deviation exceeded an empirically set threshold, a period of oscillatory bursting was declared and its duration recorded.

2.8. Calculating work exerted by a hair bundle

Data analysis, all performed in Matlab, consisted of first smoothing X for each discrete driving frequency and amplitude with a rectangular moving average, the width of which was equal to one-tenth the period of the driving frequency. We then interpolated these data to allow for an integer number of data points per period of motion. For each driving frequency and amplitude, we calculated X over an average period of motion then performed this same process for the recorded motion of the fiber's base, Δ. These data were then used to calculate on an average-cycle basis the amount of work performed by the stimulus fiber (W_{SF}), as well as the amount of energy dissipated by viscous drag (W_D). In a passive condition, these two values should sum to zero; when they sum to a negative value, we infer that the hair bundle has actively contributed work (W_A) to account for the difference (Martin and Hudspeth, 1999):

$$\overline{W}_{SF} + \overline{W}_D + \overline{W}_A = 0 \tag{8}$$

To estimate W_{SF}, we first calculated the force F_{SF} exerted by the stimulus fiber as its calibrated stiffness K_{SF} multiplied by its flexion (Martin and Hudspeth, 1999):

$$F_{SF} = K_{SF} \bullet (\Delta - X) \tag{9}$$

Multiplying F_{SF} by the velocity of the hair bundle yields the power delivered by the fiber, P_{SF} (Martin and Hudspeth, 1999):

$$P_{SF} = F_{SF} \bullet \frac{dX}{dt} \tag{10}$$

Integrating P_{SF} with respect to time over the entire average cycle of motion, or integrating the area within the curve $F_{SF}(X)$, results in W_{SF} (Martin and Hudspeth, 1999):

$$\overline{W}_{SF} = \oint F_{SF} \bullet dX = \oint P_{SF} \bullet dt \tag{11}$$

Calculating the work performed by hydrodynamic drag, W_D, followed a similar procedure but took into account higher modes of motion of the stimulus fiber. The two hydrodynamic drag coefficients ξ_{SFTip} and ξ_{SFBase} related the velocities of respectively, the fiber's tip X and base Δ to the expected drag force F_D exerted on the hair bundle (Bormuth et al., 2014):

$$\xi_{SFTip} = \frac{33}{35} \bullet \xi_{SFLorentzian} \quad \text{and} \quad \xi_{SFBase} = \frac{39}{70} \bullet \xi_{SFLorentzian} \tag{12}$$

These two coefficients were used to calculate F_D as follows (Bormuth et al., 2014):

$$F_D = -\frac{dX}{dt} \bullet (\xi_{SFTip} + \xi_{HB}) - \frac{d\Delta}{dt} \bullet \xi_{SFBase} \tag{13}$$

Multiplying F_D by the velocity of the hair bundle yields the power of hydrodynamic dissipation, P_D (Martin and Hudspeth, 1999):

$$P_D = F_D \bullet \frac{dX}{dt} \tag{14}$$

Integrating P_D with respect to time over the entire average cycle of motion, or integrating the area within the curve $F_D(X)$, results in W_D (Martin and Hudspeth, 1999):

$$\overline{W}_D = \oint F_D \bullet dX = \oint P_D \bullet dt \tag{15}$$

3. Results: spontaneous oscillations by hair bundles of the lamprey

3.1. Introduction

Spontaneous hair-bundle oscillations – being unprompted by the external environment – are not thought to assist turtles in listening for the approach of a predator, skinks in eavesdropping on alarm calls, or bullfrogs in assessing their neighbors' locations. There is no evidence that these movements, in themselves, are adaptive. Instead, spontaneous hair-bundle motility is an epiphenomenon of the active process that allows tetrapod vertebrates to spectrally analyze faint sounds amidst background noise. In this way, spontaneous oscillations are tremendously useful to the biologist seeking to study an animal's auditory system. First, because spontaneous oscillations stem from the same mechanism that drives active amplification of sounds, studying these movements can identify the molecular structures responsible for amplification. Second, because spontaneous hair-bundle oscillations derive from the complex interaction of structures in the hair bundle, these movements provide a rich indicator of a hair cell's health *in vitro*. These movements require intact tip links, which are easily broken during dissection; they reflect the cell's capacity for extruding and buffering Ca^{2+}, which can be overwhelmed if the cell is bathed in an inappropriate saline solution; and they suggest the cell is producing ATP sufficient to power the cycling of myosin motors. Therefore, we were

eager to learn whether lamprey hair bundles can undergo spontaneous oscillations – if so, these movements would form the subject of our mechanistic studies.

3.2. Physiological preparation

Visualizing and manipulating hair bundles of the lamprey's inner ear required opening the ear, obliterating the ionic microenvironment therein. We needed, therefore, physiological saline solutions that sufficiently emulated native ionic conditions.

Because the extracellular concentration of Ca^{2+} bears critically on adaptation, transduction, and spontaneous motility in tetrapod hair cells (Crawford et al., 1991; Walker and Hudspeth, 1996; Lumpkin et al., 1997; Martin et al., 2003; Manley et al., 2004), we presumed the concentration of this cation might be similarly important for lamprey hair cells. Furthermore, tetrapod hair cells *in vivo* separate two distinct ionic compartments: their apical hair bundles project into a high-K^+, low-Na^+, low-Ca^{2+} endolymph, and their basolateral aspect contacts a low-K^+, high-Na^+, high-Ca^{2+} perilymph (Bosher and Warren, 1968; Bosher and Warren, 1978; but see Runhaar and Manley, 1987). Only through experimental mimicry of this arrangement do tetrapod hair bundles reliably undergo spontaneous oscillations (Martin and Hudspeth, 1999). Therefore, we needed to determine if lamprey hair cells require an analogous "two-chamber" system.

To directly measure the concentration of Ca^{2+} bathing lamprey inner-ear hair cells *in vivo*, we made recordings from *L. appendix* ears with Ca^{2+}-sensitive microelectrodes. Recordings from seven ears revealed the presence of a low-Ca^{2+} compartment, which always bore a positive voltage relative to the external solution bathing the ear. Furthermore, in many cases repositioning the electrode revealed a distinct compartment

containing a Ca^{2+} concentration 3-40 times greater than that seen in the low-Ca^{2+} compartment and very little voltage difference relative to the bath (Table 3.1). To preserve any delicate partitions in the ear, we performed these measurements without removing the opaque cartilaginous capsule encasing the ear, directing the electrode through a small hole made in the capsule. This precluded direct visualization of the sites from which each measurement was made. To address this uncertainty, we performed an additional experiment in which one barrel of the electrode, normally dedicated to measuring Ca^{2+}, was filled with Alcian blue, while the other barrel remained dedicated to its usual task of recording the extracellular voltage at its tip. Upon detection of a significant positive voltage, we presumed to have hit the low-Ca^{2+} compartment and proceeded to pressure-inject Alcian blue (Table 3.1, last row). After fixation, we saw faint blue labeling of structures in the ventral macula, specifically the structures thought homologous to the lagena (Figure 3.1 A) and saccule (Figure 3.1 B).

Observations of *L. appendix* ears in various states of dissection assured us that the spaces overlying the lagena, saccule, and utricle *in vivo* are continuous with one another, providing our working assumption that a low concentration of Ca^{2+} is appropriate for the physiological saline solution, termed endolymph, that bathes the apical surfaces of *ex vivo* utricular hair cells. Furthermore, we decided to mimic the compartmentalization apparent in our measurements by mounting the dissected utricular epithelium in a two-compartment system, filling the basolateral compartment with a higher-Ca^{2+} saline solution, termed perilymph. Starting with the Ca^{2+} concentration ranges provided by the ion-sensitive microelectrode recordings, we empirically settled on 40 – 50 μM Ca^{2+}

endolymph and 1 mM Ca^{2+} perilymph. With this established, we set out to characterize the mechanical activity of lamprey hair bundles.

Table 3.1. Ca^{2+}-sensitive microelectrodes indicate the presence of a low-Ca^{2+} compartment in the lamprey ear that always displayed a positive voltage relative to the external solution bathing the ear. A distinct compartment was found bearing a Ca^{2+} concentration 3 – 40 times greater than that seen in the low-Ca^{2+} compartment, and very little voltage difference relative to the bath. There is no linear correlation between Ca^{2+} concentration and voltage in the positive voltage compartment ($R^2 = 0.003$) and no linear correlation between Ca^{2+} concentrations in the two compartments of a given ear ($R^2 = 0.01$).

	Low-Ca^{2+} compartment		**High-Ca^{2+} compartment**	
arbitrary ear #	**Ca^{2+} (µM)**	**voltage re bath (mV)**	**Ca^{2+} (mM)**	**voltage re bath (mV)**
1	40	+ 17	1.6	0
2	50	+ 9	0.8	+ 2
3	58	+ 6	1.1	0
4	88	+ 6.5	-	-
5	320	+ 11	0.8	+ 0.5
6	330	+ 15	-	-
7	420	+ 5.5	1.3	0
8	- Alcian injection-	+ 8	-	-

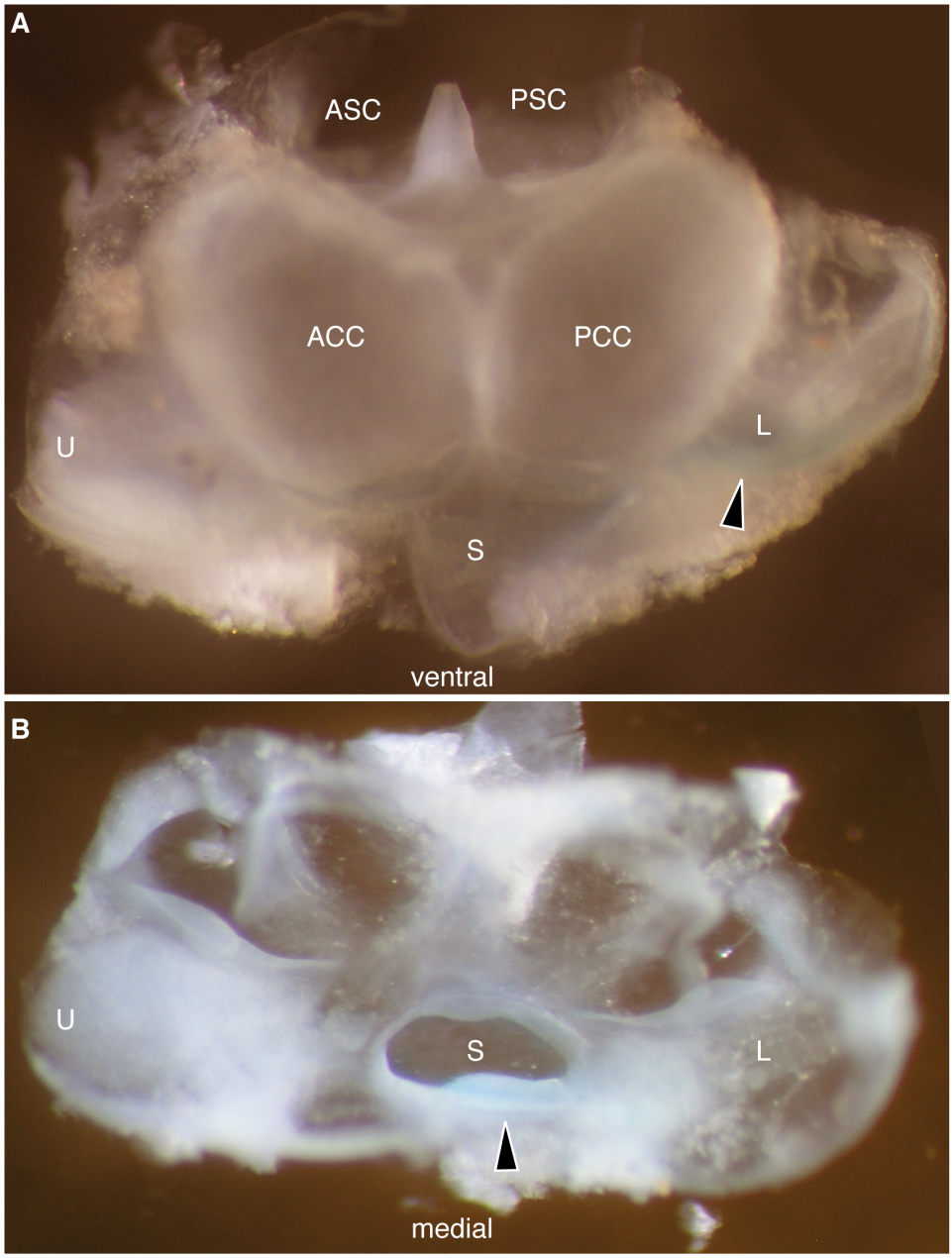

Figure 3.1. Alcian Blue staining suggests the low-Ca^{2+}, high-voltage compartment is bounded by the ventral macula. **A.** Medial view of a fixed right ear. Staining is most apparent on the ventral surface of the lagena (arrowhead). **B.** Dorsal view of the same ear after dissecting away dorsal structures. Staining is most apparent on medial wall of saccule (arrowhead). Utricle (U), saccule (S), lagena (L), anterior and posterior ciliated chambers (ACC and PCC respectively), dorsal aspect of the anterior (ASC) and posterior (PSC) semicircular canals. The ear is approximately 1mm long along its anteroposterior axis.

3.3. Spontaneous oscillations and their underlying basis

Given that lamprey hair cells had never been studied physiologically, we began our work with no expectation of whether their hair bundles would undergo spontaneous oscillations. In the face of this uncertainty, it was helpful to have direct knowledge of the native Ca^{2+} concentrations in the lamprey ear. We next needed to determine which population of inner-ear hair cells on which to focus our observations.

The utricle was chosen for physiological studies because its epithelium is flatter than that of the sacculus and because it is larger than the lagena, containing more than a thousand hair cells (Figure 3.2 B). These hair cells have an apical surface about 2 μm in diameter, and their bundles can be up to 10 μm tall (Figure 3.2 B).

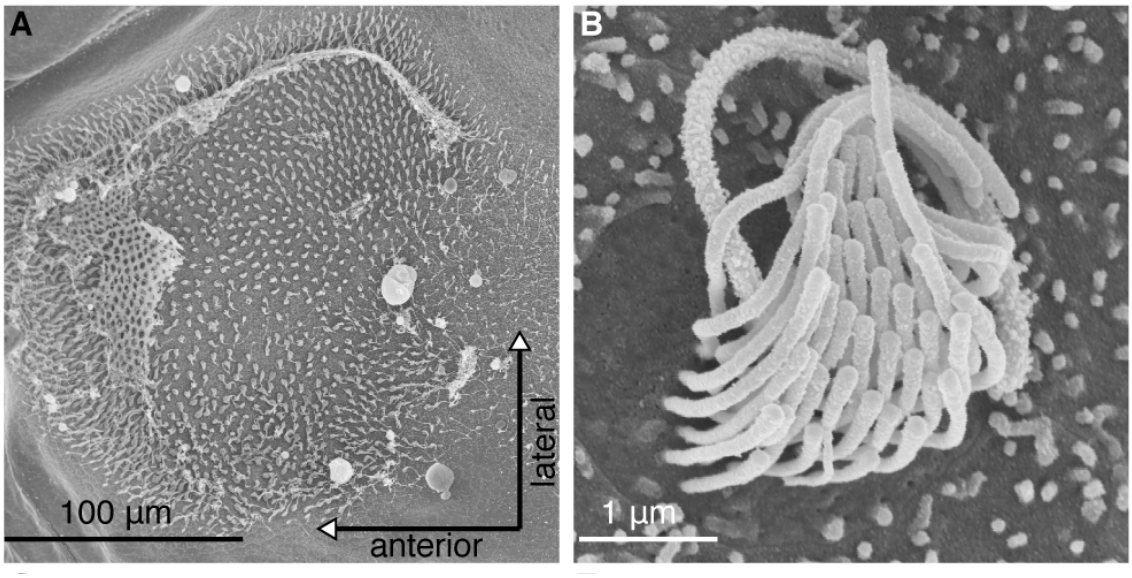

Figure 3.2. The lamprey hair bundles on which this study focuses. **A.** A scanning electron micrograph of the anterior-most endorgan of the *Petromyzon marinus* macula communis. We consider this endorgan homologous to the gnathostome utricle (Lowenstein et al., 1968; Hammond and Whitfield, 2006). Portions of the otolithic membrane remain atop these hair bundles, at the anterior portion of this organ. **B.** A scanning electron micrograph of one *P. marinus* utricular hair bundle, its tallest edge oriented toward the top left of the figure.

After establishing appropriate endolymph and perilymph recipes, we observed large-amplitude spontaneous oscillations in *L. appendix* (Figure 3.3). These oscillations were qualitatively similar to the spontaneous oscillations of bullfrogs: they consisted of abrupt transitions between slowly varying states, with their dominant frequency of oscillation below 20 Hz and their root-mean-square amplitudes roughly 100 nm (Figure 3.4 A). As the consistency of the dissection efforts improved, we often saw preparations in which hundreds of utricular hair bundles oscillated for tens of minutes. Using the same physiological saline solutions as for *L. appendix*, we also observed spontaneously oscillating hair bundles in the utricles of *P. marinus* (Figure 3.4 B).

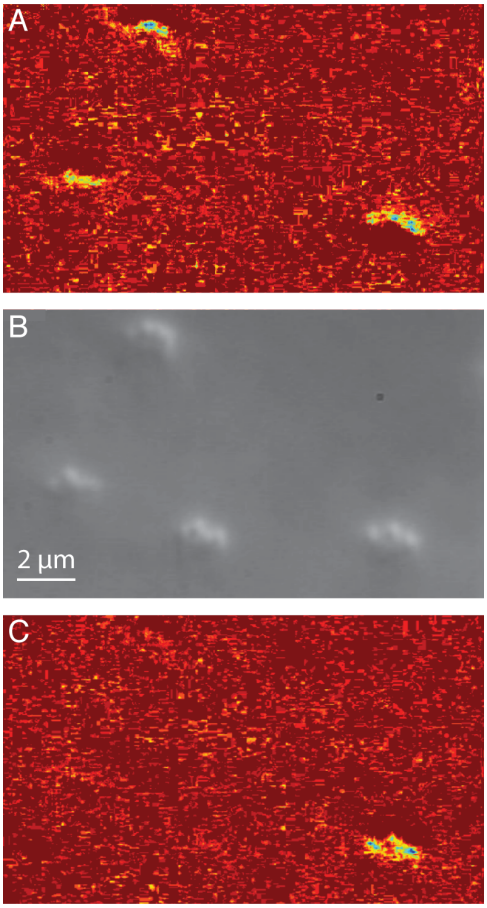

Figure 3.3. Spontaneous oscillation of hair bundles from the *L. appendix* utricle. The middle panel **B** shows a frame from a video of four hair bundles; as in figure 3.2, the epithelium is viewed along its apical-basal axis. All four hair bundles' taller edges are oriented toward the top of the image. Subtracting from this frame the preceding frame yields the false-color image in **A**, revealing that the two left-most hair bundles each moved toward their shorter edges, while the right-most hair bundle moved toward its taller edge. **C.** Subtracting that same frame from its following frame then revealed a movement of the right-most hair bundle toward its shorter edge. This method of analyzing still frames of hair-bundle oscillations is taken after Martin (2003).

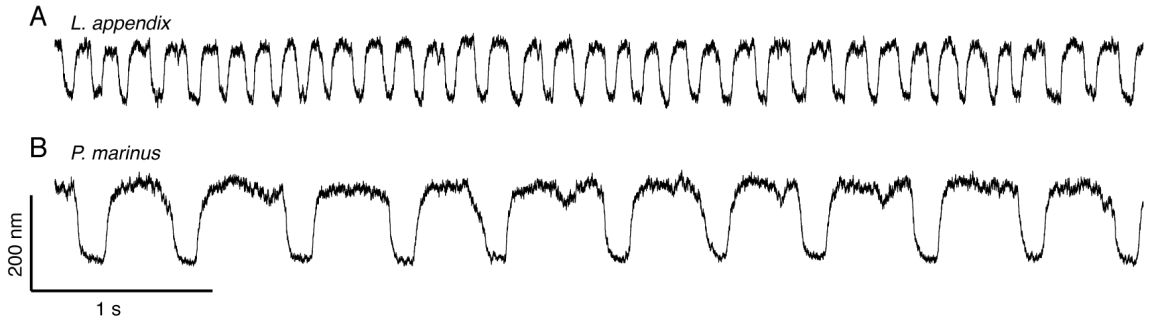

Figure 3.4. Displacement records of two spontaneously oscillating utricular hair bundles, from **A.** *L. appendix* and **B.** *P. marinus*. Upward deflections denote movements toward the bundle's taller edge.

3.3.A. Sensitivity to external Ca^{2+} concentration

After demonstrating that lamprey hair cells oscillate spontaneously, we considered whether hair-bundle motility evolved before the split between jawless and jawed vertebrates. Specifically, we hypothesized that lamprey spontaneous oscillations stem from molecular mechanisms homologous to those underlying spontaneous oscillations in tetrapods: stereociliary myosin motors interacting with the gating of transduction channels. To test this, we focused our efforts on one lamprey species, *L. appendix*.

Given the established effects of Ca^{2+} on the hair-bundle adaptation motors of some tetrapod species (Eatock et al., 1987; Crawford et al., 1991; Walker and Hudspeth, 1996; Cyr et al., 2002), we predicted that iontophoretic control of the Ca^{2+} concentration in the vicinity of an oscillating lamprey hair bundle would alter the residence time in the positive state of these oscillations. Indeed, we consistently found in 11 utricular cells that the mean positive residence time could fall roughly twofold over a physiological range of tested Ca^{2+} concentrations, with slight or variable effects on the negative residence time

(Figure 3.5). This effect held whether the iontophoretic currents were presented in ascending (Figure 3.5, left) or descending order (Figure 3.5, right).

It seemed possible that the effect described above could be due to the passage of current by the iontophoresis electrode, rather than the increase of Ca^{2+} delivered by that current. To address this, we performed a control in which the iontophoresis pipette was filled with 120 mM KCl rather than the usual 120 mM $CaCl_2$. The expected result of passing positive current in this condition is a local increase in K^+ concentration, with no significant change in Ca^{2+}. Because the concentration of K^+ in the artificial endolymph bathing the bundles is more than 100 mM, an increase of a few tens of micromolar should yield negligible effects on a hair bundle. We found that the waveform of lamprey spontaneous oscillations was not appreciably affected by the mere passage of positive iontophoretic currents (Figure 3.6).

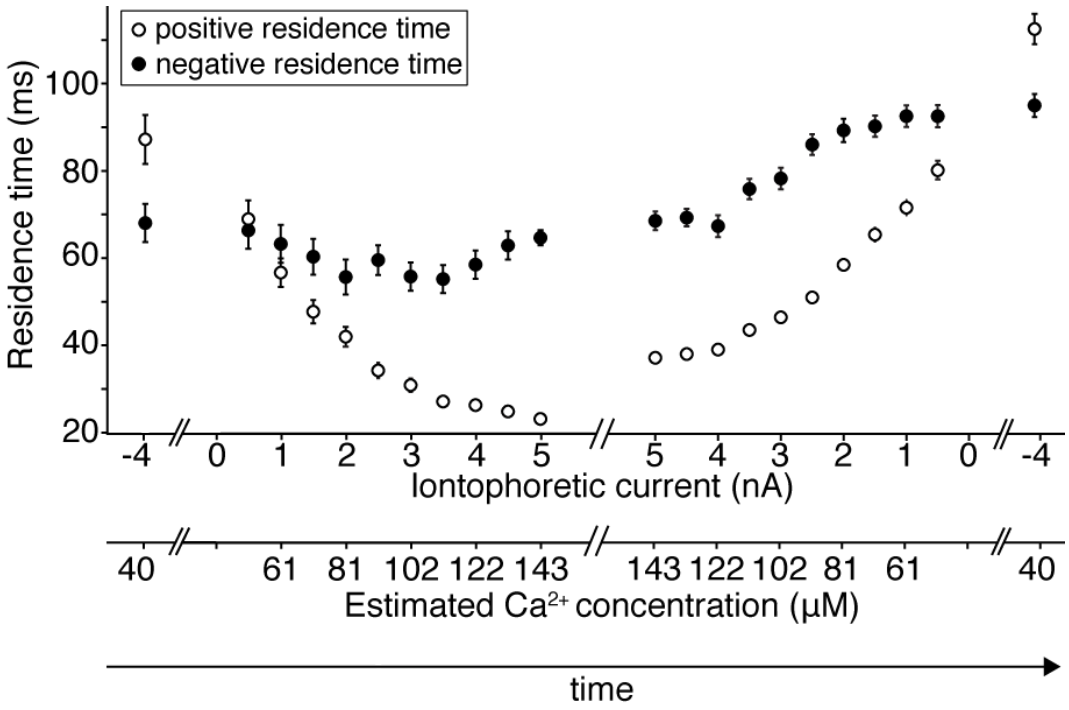

Figure 3.5. Increasing extracellular Ca^{2+} by iontophoresis shortens the positive residence time of *L. appendix* spontaneous oscillations. A hair bundle oscillated throughout a series of incremental changes in iontophoretically applied Ca^{2+}. From ten seconds of motion at each iontophoresis step, the mean positive residence time (open circles) and mean negative residence time (filled circles) were calculated. Error bars denote SEM; for many points, the size of the symbol exceeds that of the error bar. The series of iontophoresis steps was first delivered in ascending order, then several minutes later in descending order. For baseline measurements, a holding current of -4 nA was applied to prevent diffusive release of Ca^{2+}. In view of the strongly nonlinear relationship between holding currents and cation release, the abscissse are broken between the holding current and positive ejection currents. The floating abscissa denotes the estimated steady-state Ca^{2+} concentrations achieved by each current magnitude. This hair bundle was in the anterolateral region of the utricle, with its taller edge oriented medially. The iontophoresis pipette was positioned 3 μm from the shorter edge of the hair bundle.

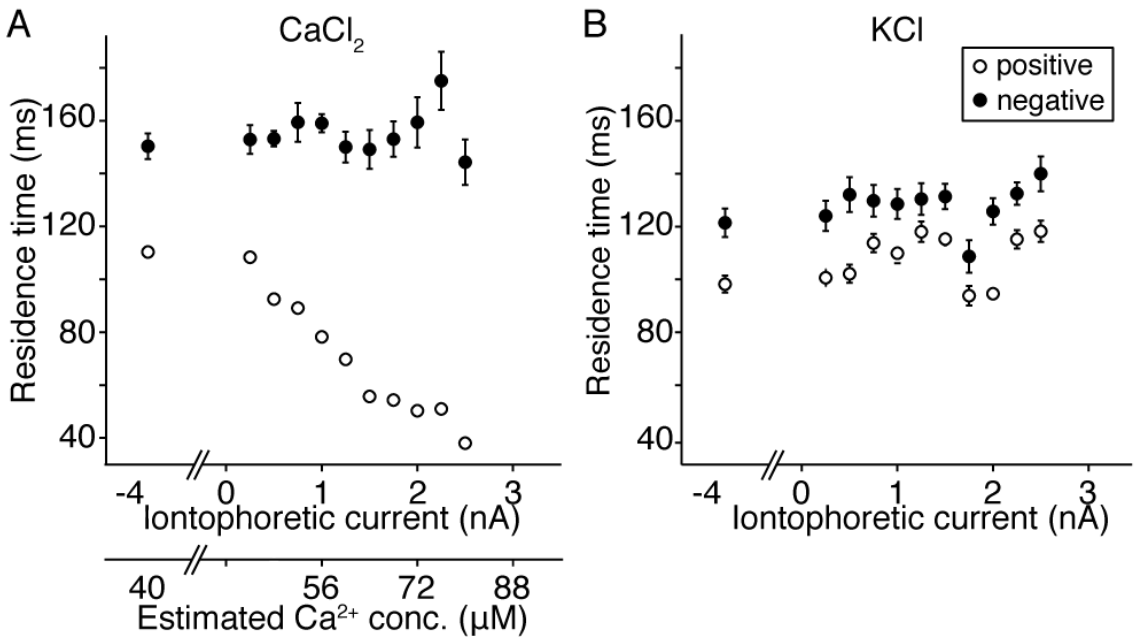

Figure 3.6. The effect of Ca^{2+} on *L. appendix* positive residence time is not an artifact of passing current. A. Iontophoresing Ca^{2+} onto a hair bundle shows that higher extracellular Ca^{2+} concentrations reduce the positive residence time of this lamprey hair bundle's spontaneous oscillations. **B.** Several minutes later, iontophoretic currents borne by a different cation, K^+, yielded no such effect on the same hair bundle. In each case, the tip of the iontophoresis pipette was 4 μm from the hair bundle. Each data point was calculated from ten seconds of spontaneous oscillation. Error bars denote SEM; for many points, the size of the symbol exceeds that of the error bar. A holding current of -4 nA was applied to prevent diffusive release of each cation; in view of the strongly nonlinear relationship between holding currents and cation release, the abscissa is broken between the holding current and positive ejection currents. The floating abscissa denotes the estimated steady-state Ca^{2+} concentrations achieved by each current magnitude.

The key strength of iontophoresis is the temporal control it affords, permitting our presentation of many Ca^{2+} concentrations in a short amount of time, before slower-timescale processes such as the exhaustion of the hair cell's ATP stores could appreciably alter the data. The primary weakness of iontophoresis is a slight uncertainty in the steady-state concentrations achieved, especially for minute ejection voltages (Purves, 1981). Though vastly slower than iontophoresis, manual exchange of the solution provides more accurate control of the Ca^{2+} concentration bathing the hair bundles. Using this mode of Ca^{2+} manipulation, the same effect of Ca^{2+} on spontaneous oscillations was seen in 12 cells (Figure 3.7).

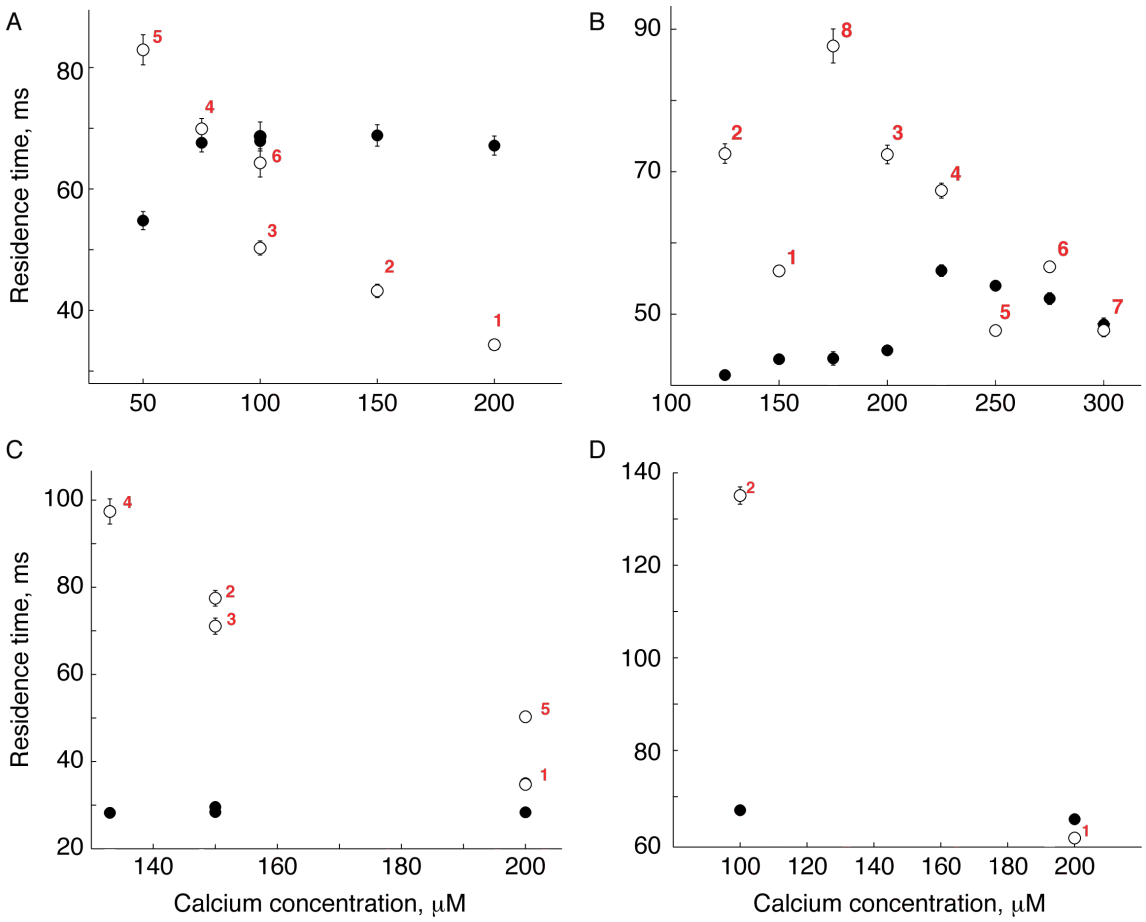

Figure 3.7. Manual exchange of endolymph solutions corroborates iontophoretic data. Shown are data from four representative cells from the *L. appendix* utricle. At each concentration tested, 30 seconds of spontaneous oscillations were recorded, from which were calculated the mean positive residence time (open circles), and mean negative residence time (filled circles). Bars describe S.E.M. and red numbers accompanying open data points indicate the order of solution presentation. Consecutive recordings were taken approximately three minutes apart.

3.3.B. The effects of myosin inhibitors

The above results with Ca^{2+} are consistent with a myosin powering the spontaneous oscillations of lamprey hair cells. However, myosins are certainly not the only molecular motors known to be regulated by this cation; dynein, which ultrastructural studies suggest is present in the kinocilia of some lamprey hair cells (Katori et al., 1994), can also be regulated by intraciliary Ca^{2+} levels (Smith, 2002). To further test our hypothesis of molecular homology between lamprey and tetrapod spontaneous oscillations, we examined the effects of two known myosin inhibitors – one broadly acting, the other targeted to a specific myosin class. In both cases, we predicted the inhibitor to attenuate or halt spontaneous oscillations.

First, we tested the effect of butanedione monoxime (BDM) on lamprey spontaneous oscillations. With a relatively high IC_{50} of 5 mM, BDM inhibits force production by class II myosins by impeding phosphate release, biasing these ATPases toward their weak actin-binding state (Herrmann et al., 1992). Despite uncertainty about its action on class I myosins, it is clear that BDM can reduce the open probability of the transduction channels of turtle cochlear hair bundles (Wu et al., 1999). This is consistent with BDM inhibiting the myosin(s) responsible for adjusting the resting tension in gating springs. This drug was later shown to reversibly inhibit spontaneous oscillations of bullfrog saccular hair cells (Martin et al., 2003). Despite this drug having uncharacterized effects on class I myosins, as well as potential off-target effects at its effective dose, the historical use of this drug in tetrapod hair cells provided a rationale for testing its effects on lamprey in this comparative study.

Spontaneous oscillations were inhibited by the application of BDM in 13 of the 14 hair cells studied. Of these 13, four cells resumed oscillating after BDM washout

(Figure 3.8). Our finding that lamprey hair-bundle oscillations are halted by BDM, and often reversibly so, agrees with that from the bullfrog (Martin et al., 2003).

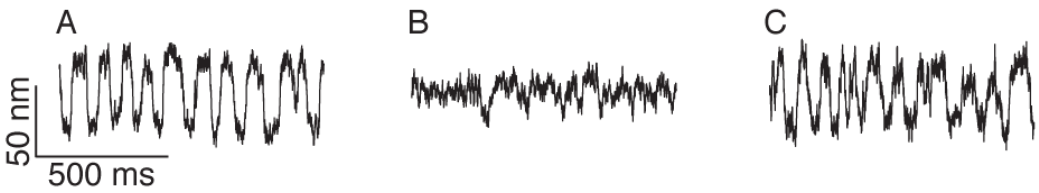

Figure 3.8. Butanedione monoxime reversibly interferes with spontaneous oscillations of *L. appendix* utricular hair bundles. Shown are three one-second recordings of hair-bundle motion; upward deflections correspond to the bundle moving toward its taller, positive edge. **A.** A control recording in regular endolymph reveals a bundle initially oscillating at 9.6 Hz. **B.** While bathed in 5 mM BDM, oscillations were attenuated, with no peak detectable in the power spectrum of hair-bundle motion. **C.** After washout of BDM, the oscillations returned to a frequency of 9.1 Hz with an rms magnitude of 19 nm. This result is representative of 4 cells.

The results with BDM further supported the role of a myosin in powering lamprey spontaneous oscillations. To query the involvement of class I myosins in particular, we tested the effect of extracellularly applied pentachloropseudilin (PClP) on these movements. PClP reversibly inhibits the *in vitro* ATPase activity of class I myosins with an IC_{50} of 1-5 μM while affecting the activity of other myosins (families II and V) with an IC_{50} of greater than 90 μM (Chinthalapudi et al., 2011). To our knowledge, the present study marks the first experiments with PClP on hair cells, so it was reassuring that the drug has already been shown in cultured HeLa cells to disrupt functions known to rely on myosin Ic in the late endosomal pathway.

To our surprise, four of four lamprey hair cells bathed in 10 μM PClP continued their spontaneous oscillations for more than 30 minutes (Figure 3.9 A). Any subtle changes in their waveform were not differentiable from those evoked by exposure to DMSO alone. To place this result in a comparative framework, we then tested this drug on spontaneously oscillating bullfrog hair cells. In 32 of 35 bullfrog hair cells bathed in 2.5 – 5 μM PClP, spontaneous oscillations were halted within minutes. Of these, 14 cells provided at least one recording of spontaneous oscillations before their eventual arrest. These recordings displayed an increased residence time in the bundles' negative position (Figure 3.9 B).

To compare all the cells' responses to PClP, we calculated the average negative and positive residence times (Figure 3.10). Plotting these values with respect to time exposed to the drug underscored the fact that most bullfrog hair cells cease oscillating in PClP much more rapidly than do those of the lamprey. Second, this analysis showed that bullfrog hair cells often underwent a 10 – 60 fold increase in their oscillations' negative residence time in less than 10 minutes. On the other hand, lamprey hair cells displayed at most a 2-fold increase in their negative residence time over the tens of minutes they continued oscillating in the drug (Figure 3.10A). Bullfrog hair cells generally experienced a decrease in the average positive residence time of their oscillations, whereas only one of the four lamprey hair cells showed this effect (Figure 3.10 B).

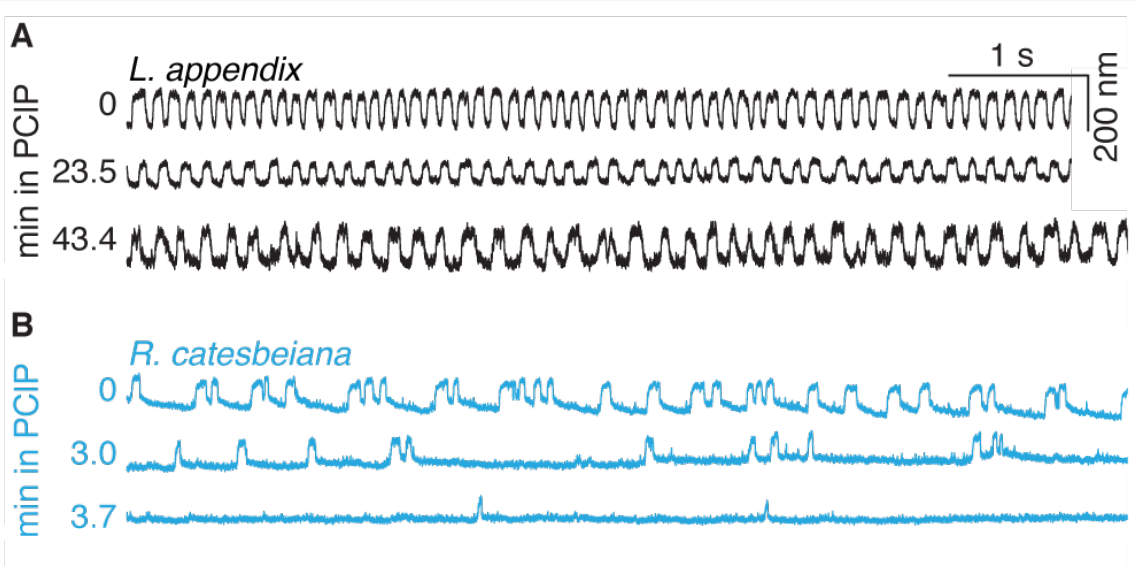

Figure 3.9. *L. appendix* spontaneous oscillations, in contrast to bullfrogs', are not halted by PClP, an inhibitor specific to class-I myosins. A. Recordings from a spontaneously oscillating lamprey hair cell in 1% DMSO (top) and after 23.5 and 43.4 minutes in 10 μM PClP carried by 1% DMSO (middle and bottom respectively). Representative of 4 of 4 lamprey hair cells whose oscillations persisted for more than 30 minutes during exposure to PClP. **B**. Recordings from a spontaneously oscillating bullfrog saccular hair cell in 0.5% DMSO (top) and after 3.0 and 3.7 minutes in 5 μM PClP carried by 0.5% DMSO (middle and bottom respectively). Representative of 32 of 35 bullfrog hair cells whose oscillations were arrested in PClP, and of the subset of 14 cells whose oscillations persisted long enough to be recorded in the presence of the drug.

Because PClP has been shown to reduce the coupling of class I myosins to actin, we surmised that bullfrog hair cells treated with the drug may display an inverse correlation between the fold changes of their positive and negative residence times. When we plotted the change in positive residence time as a function of the change in negative

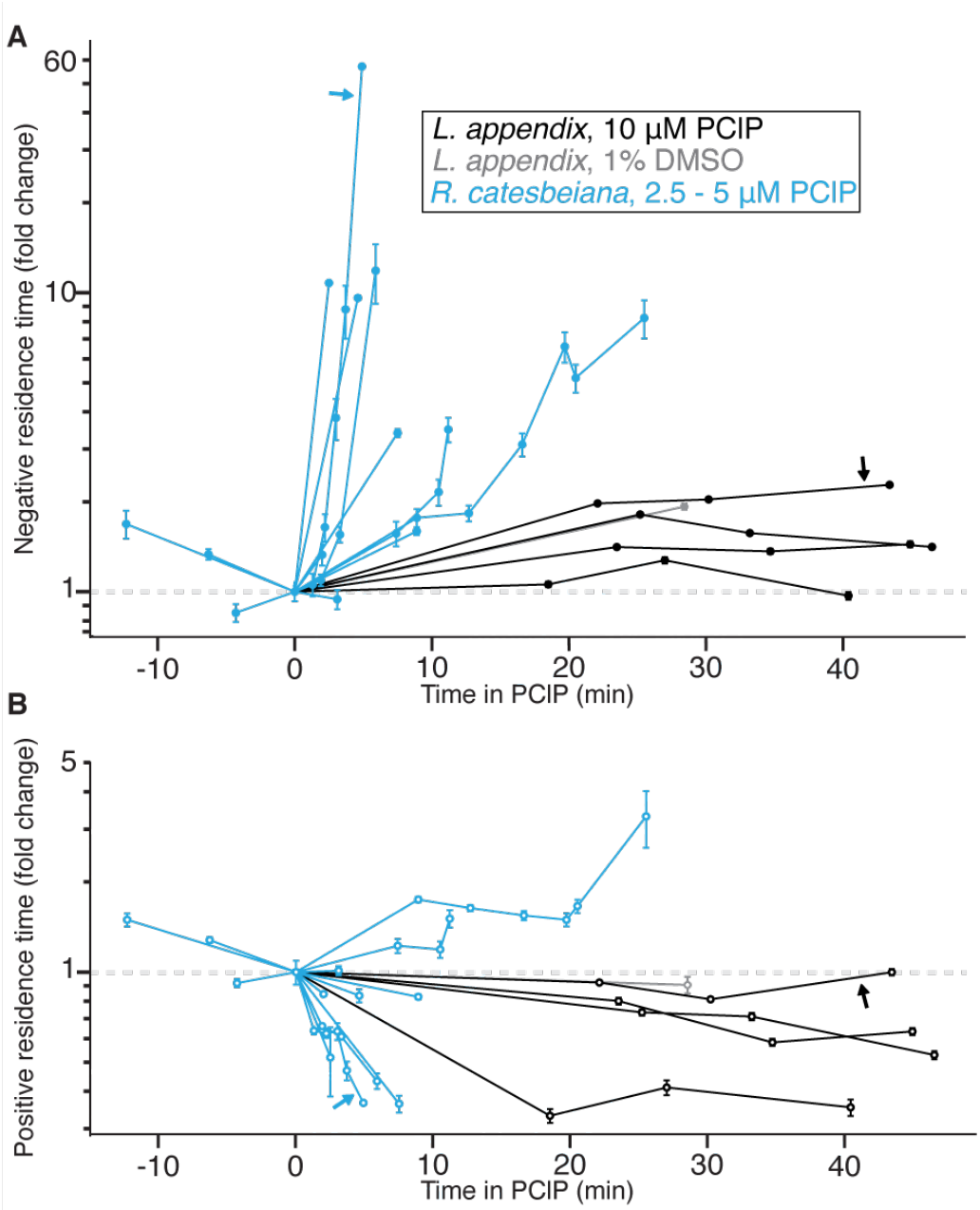

Figure 3.10. Prior to their arrest in PClP, spontaneous oscillations by bullfrog hair bundles undergo a change in waveform, an effect not apparent in *L. appendix*. A. Fold change in the negative residence time of lamprey (black, 4 cells) and bullfrog (blue, 10 cells) spontaneous oscillations as a function of time spent in PClP. Note log scaling of ordinate. Arrows indicate the two cells whose raw data were shown in Figure 3.8. Shown for comparison is a lamprey hair cell in 1% DMSO alone (gray). **B**, Fold change in the positive residence time from the same 11 recordings depicted in (**A**); note change in ordinate.

residence time we indeed saw that, for most oscillating bullfrog hair cells, lengthening of the negative residence time was related to an abbreviation of their mean positive residence time (Figure 3.11 A). Lamprey hair cells, on the other hand, showed no correlation between these two aspects of their spontaneous oscillations. For instance, the cell that showed the most shortening of its positive residence experienced almost no change in its negative residence time (Figure 3.11 B).

We were curious about the two bullfrog hair cells that defied the trend by showing an unexpected positive correlation between the change in negative and positive residence times (Figure 3.11 A). Unlike the others, these two cells retained a high degree of multimodality throughout their exposure to this drug (Figure 3.11 C). Multimodal oscillations are characterized by periods of oscillatory bursting, interspersed with relaxations toward the bundle's shorter edge (Shlomovitz et al., 2013). We realized that the calculation of positive and negative residence times does not reveal the duration of oscillatory bursts (Figure 3.11 C, dark green). Furthermore, we wanted to analyze the long periods of quiescence at negative displacements (Figure 3.11 C, dark purple) separately from the brief negative excursions within oscillatory bursts (Figure 3.11 C, magenta). Therefore, for the two bullfrog cells whose oscillations remained multimodal, we performed an additional analysis, calculating the mean durations of quiescence and oscillatory bursting before and during exposure to PClP. For both cells, the oscillatory bursts became shorter in the presence of the drug, falling to about 25% of the duration in DMSO alone (Figure 3.11 D, dark green). Also, for both cells the quiescent phases lengthened, reaching about three times the length of their duration in DMSO alone (Figure 3.11 D, dark purple).

Figure 3.11. For bullfrog hair cells whose spontaneous oscillations are multimodal, PClP shortens the duration of oscillatory bursting even when it fails to shorten the positive residence time. A. Each line depicts data from a single oscillating bullfrog hair bundle over time; the fold change in positive residence time is plotted as a function of fold change in negative residence time. The recordings were those considered in Figure 3.10. Two cells (marked with arrowheads) displayed a positive correlation between these quantities. Log-log scaling was used to better convey the more densely populated areas of the plot. **B.** The same analysis of four lamprey hair bundles, with the same scaling but a truncated abscissa. **C.** Several seconds of multimodal oscillation from the hair bundle whose data is marked with an open arrowhead in (**A**), showing three bouts of oscillatory bursting (dark green) interrupted by periods of quiescence (dark purple). Oscillatory bursts are comprised of abrupt transitions between positive ("p," light green) and negative ("n," magenta) states. **D.** For two bullfrog hair cells whose oscillations were multimodal, the changes in duration of quiescence (dark purple) and of oscillatory bursting (dark green) are plotted as functions of the time spent in 5 μM PClP. Arrowheads (filled and open) indicate these cells' corresponding analyses in (**A**). Error bars denote SEM; each point was calculated from 30 seconds of spontaneous oscillation.

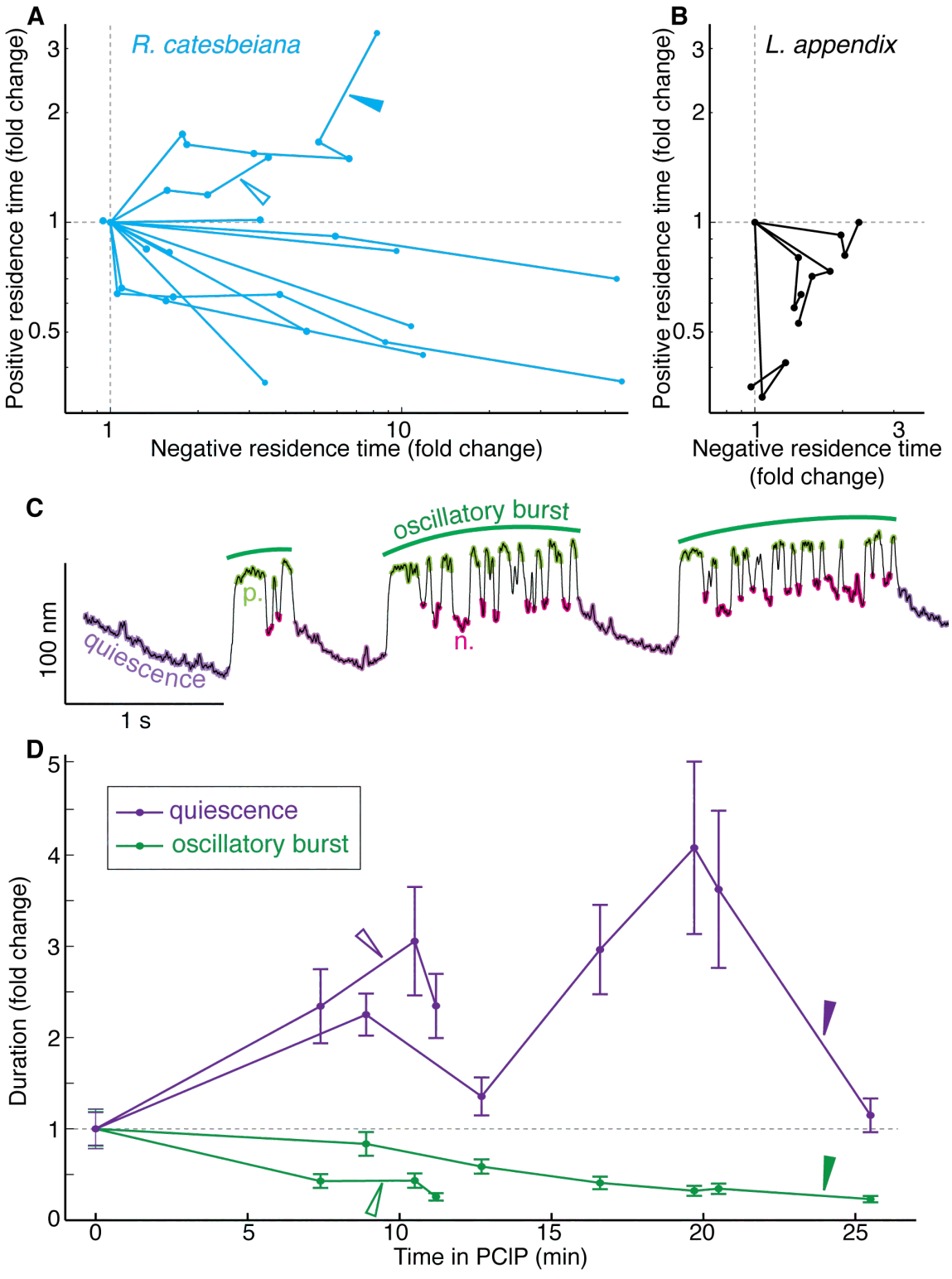
A
R. catesbeiana
Positive residence time (fold change)
Negative residence time (fold change)
B
L. appendix
Positive residence time (fold change)
Negative residence time (fold change)
C
oscillatory burst
p.
n.
100 nm
quiescence
1 s
D
quiescence
oscillatory burst
Duration (fold change)
Time in PCIP (min)

Figure 3.11

3.3.C. Sensitivity to a transduction-channel blocker

The active process of tetrapods requires the interaction of two general components: stereociliary myosin motors and mechanotransduction channels. By adjusting the tension in gating springs, myosin-based adaptation can set the range of displacements over which transduction channels gate. In tandem with the nonlinearity caused by cooperative channel gating, this slow, active adjustment can generate spontaneous oscillations (Le Goff et al., 2005). By exploring the effects of Ca^{2+} and myosin blockers on lamprey spontaneous oscillations, as described above, we probed one of the two components of the hair-bundle active process. We next studied the second component, the gating of transduction channels, with the use of gentamicin. This aminoglycoside antibiotic has long been known to block the hair-cell transduction channels of tetrapod vertebrates (Howard and Hudspeth, 1988).

In *L. appendix*, gentamicin halted or perturbed (Figure 3.12) spontaneous oscillations in 19 of 21 cells tested. One of these non-responding cells had been oscillating irregularly in an ageing preparation, and the other was treated only with a very weak pulse of gentamicin. Some subtler effects were also apparent from these recordings. Hair bundles routinely displayed slow movements toward their negative edge during the blockade of their oscillations (Figure 3.12 A). This has been seen in bullfrog hair bundles' response to gentamicin (Martin et al., 2003) and is consistent with gentamicin blocking Ca^{2+} entry. We also noted that, when gentamicin halted oscillations, it did so by freezing the hair bundle in a positive position. When some spiky oscillations persisted (Figure 3.12 A, second and third recordings), they involved only brief excursions to a negative position; most of the time was spent in a positive position. These related

findings are consistent with gentamicin wedging transduction channels into their open configuration, as is thought to occur in tetrapod hair bundles.

Because gentamicin seemed to bias oscillating hair bundles toward their taller edges, we further studied this by incrementally increasing concentrations of gentamicin, recording ten seconds of hair-bundle motion during exposure to each dose (Figure 3.12 B). The apparent effect was quantified by calculating the fraction of time the oscillating hair bundle spent at displacements more positive than its median displacement. By this metric, gentamicin's concentration-response relation of a given hair bundle was stable over many minutes (Figure 3.13 A). All hair bundles displayed a monotonically increasing relationship between the concentration of gentamicin and the fraction of time spent above the median displacement (Figure 3.13 B).

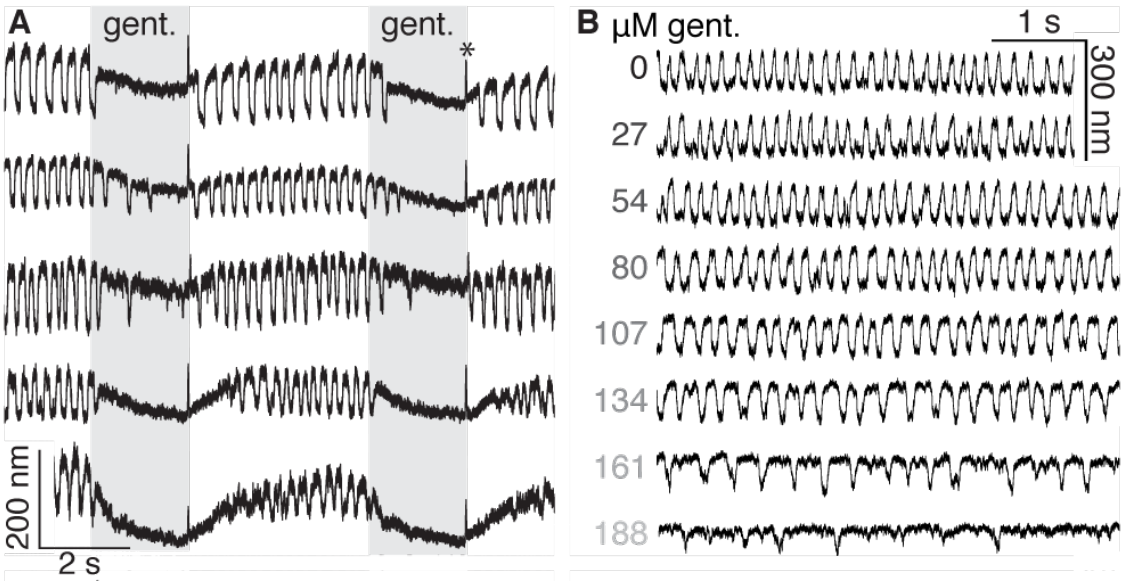

Figure 3.12. Gentamicin reversibly attenuates spontaneous oscillations in *L. appendix* hair bundles. **A**. Twelve continuous seconds of five hair bundles' spontaneous oscillations are shown. Upward deflections always denote motion toward the bundle's taller edge. Hair-bundle motion during two bouts of 10-20 µM gentamicin iontophoresis (highlighted in gray) is displayed for each cell. The rapid excursions after each gentamicin bout are calibration pulses (*). **B**. Gentamicin was iontophoresed in finely graded increments, during each of which hair-bundle motion was recorded. In these recordings from one hair bundle, each continuous recording is vertically offset from the others by an arbitrary amount. The top trace represents the response in the absence of gentamicin, and successively lower traces depict spontaneous oscillations in higher concentrations of this drug.

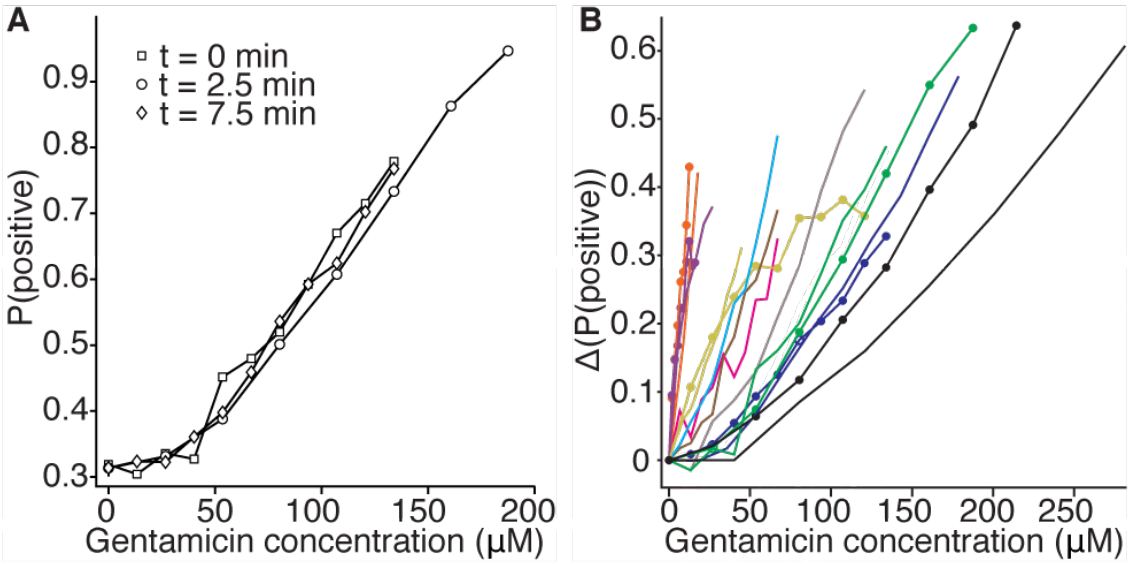

Figure 3.13. Gentamicin halts spontaneous oscillations by *L. appendix* hair bundles through concentration-dependent biasing toward the taller edge. The effect of gentamicin on spontaneous oscillation waveform was quantified by calculating "P(positive)," the fraction of time spent by an oscillating hair bundle at displacements more positive than its median displacement. **A.** Shown are three dose-response datasets from a single hair bundle, each measured several minutes apart. These data come from the same hair bundle featured in Figure 3.12 B. At sufficiently high concentrations, oscillations were halted, precluding a meaningful calculation of P(positive). **B**. To facilitate comparison across multiple hair bundles, we show here the change in P(positive) with respect to the value measured in the absence of gentamicin. The data from ten hair bundles are each plotted in a distinct color. In cases in which multiple recordings were made from one cell, the second recording is plotted with circles at each data point. Two recordings from (**A**) are plotted in green, with the third omitted for clarity.

4. Results – amplification by hair bundles of the lamprey ear

4.1 Introduction

We have shown that spontaneous oscillations occur in the utricles of two lamprey species, vertebrates quite distantly related to the tetrapods. We have also shown that in *L. appendix* these movements stem from mechanisms largely similar to those driving tetrapod spontaneous oscillations. Curious about the adaptive significance of spontaneous oscillations in lampreys, we hypothesized that these unprompted movements are a byproduct of a process used to mechanically amplify sinusoidal stimuli. To test this, we calculated the amount of mechanical work contributed by a lamprey hair bundle when its motion was entrained to periodic stimuli of different frequencies and amplitudes. Further, if we observed any hair bundles exerting positive work, we would then test whether this amplifying ability was altered by gentamicin.

4.2. Frequency-tuned mechanical work

When we adhered a stimulus fiber to a spontaneously oscillating hair bundle (Figure 4.1 A), the oscillation's amplitude was reduced and its frequency increased, but its waveform retained a pronounced limit-cycle character with fast and slow timescales of motion (Figure 4.1 B, top two traces). When the base of the probe was driven sinusoidally, the hair bundle's motion entrained to that of the stimulus; in the presence of gentamicin, this entrainment persisted, but the amplitude of motion was dramatically reduced (Figure 4.1 B, bottom two traces).

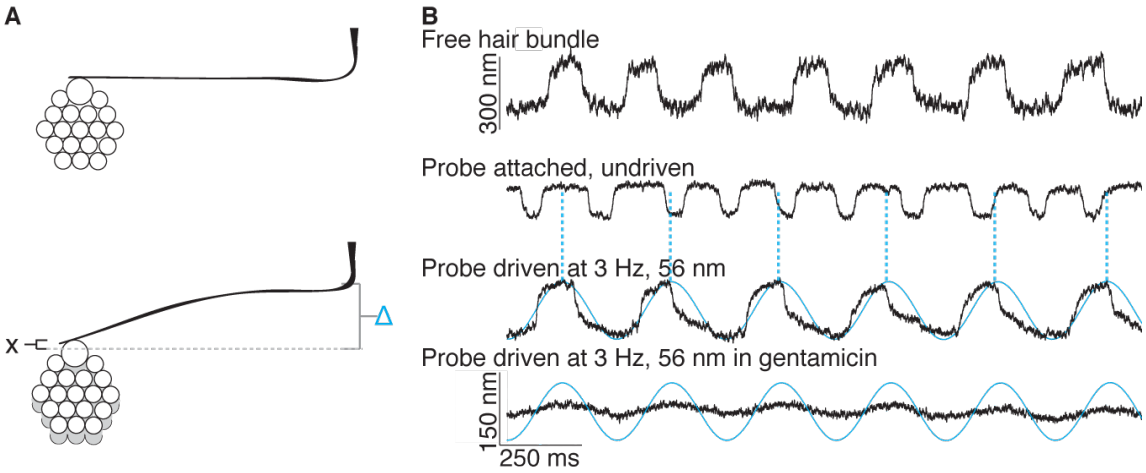

Figure 4.1. Sinusoidal stimulation of a spontaneously oscillating *L. appendix* hair bundle. A, A schematized hair bundle with the tip of a stimulus fiber attached to the kinocilium at the bundle's tallest edge (top). When a displacement command of magnitude Δ is imposed on fiber's base, the hair bundle's resultant displacement X along its axis of height gradation is measured (bottom). **B,** Four displacement recordings from a single lamprey utricular hair bundle. When unloaded, its motion showed a peak frequency of 3.8 Hz (top). The vertical scaling from this top recording differs from that of the subsequent three recordings. Attaching a stimulus fiber of stiffness 50 μN/m and drag coefficient 125 nNs/m elevated the oscillation frequency to 5.1 Hz (second from top). The base of the fiber was then driven sinusoidally (third from top). To emphasize the hair bundle's entrainment to the stimulus, broken lines guide the eye up from each period of driving stimulus to the previous, undriven, recording. The same stimulus protocol was applied to the hair bundle in the presence of gentamicin (bottom). The hair bundle's motion is depicted in black, and the motion of the probe's base in cyan. All data in Figures 4.2 and 4.3 derive from this hair bundle.

The motion of the hair bundle led that of the stimulus fiber during most cycles of motion (Figure 4.1 B, third from top), suggesting that the hair bundle was actively contributing to the system's periodic movement. To quantify this impression, we then calculated for an average cycle the active mechanical work contributed by the hair bundle, termed W_A, by calculating the work performed by the stimulus fiber (W_{SF}) and the energy lost to dissipation by hydrodynamic drag (W_D). This approach is described in greater detail in the Methods. This experiment revealed that, for the 3 Hz, 56 nm stimulus featured in Figure 4.1, W_{SF} was not only insufficient to have countered W_D, but it was negative – meaning the stimulus fiber actually impeded the motion of the bundle – for almost the entire displacement range (Figure 4.2 A, top). This result confirmed our impression that the hair bundle was actively performing mechanical work to counter viscous dissipation. At the same stimulus amplitude but a higher frequency, W_{SF} was equal and opposite to W_D, indicating that W_A was negligible under this condition (Figure 4.2 A, bottom). When W_A was similarly calculated for all frequencies and amplitudes tested, we found that this active process displays frequency tuning (Figure 4.2 B) with the highest values of work production around 3-5 Hz. The stimulus frequency evoking the highest value of W_A shifted to lower values with increasing stimulus amplitude.

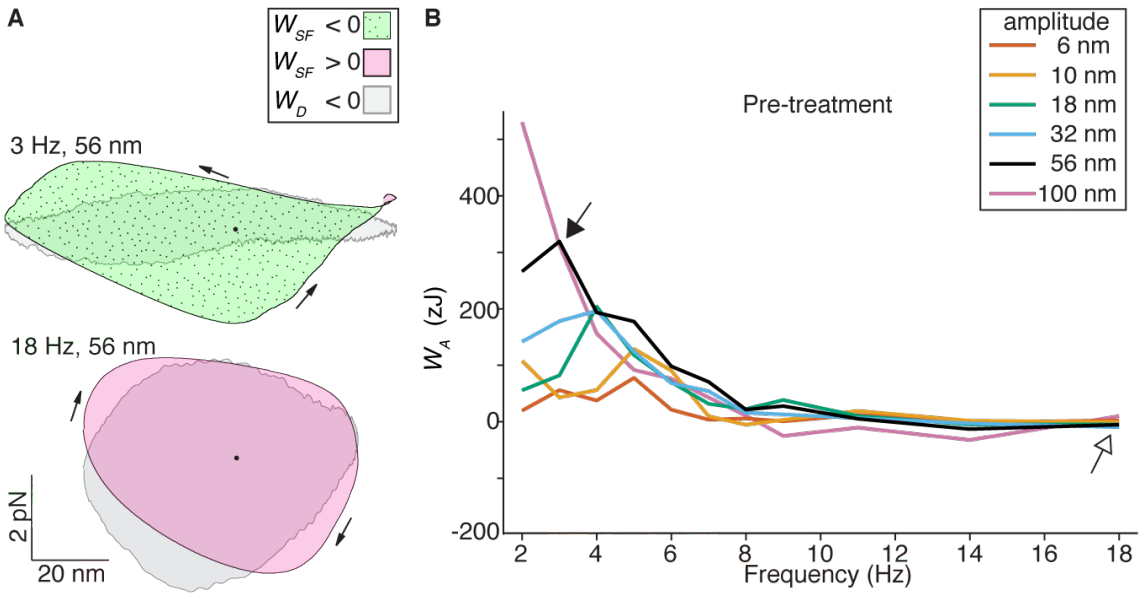

Figure 4.2. Summing the work performed by the stimulus fiber and by viscous drag reveals frequency-tuned work production by *L. appendix* hair bundles. A. For an average cycle of hair-bundle motion we plotted the force exerted by viscous drag (F_D, gray line) and the force exerted by the stimulus fiber (F_{SF}, black line) as functions of X. Because the motion was periodic the lines form loops, the enclosed areas of which show respectively the energy lost to viscous dissipation, W_D, and the work contributed by the stimulus fiber, W_{SF}. Because drag forces always oppose motion, drag loops progress counter-clockwise, lending a negative sign to the work calculated from their circumscribed area (gray shading). In contrast, forces exerted by the flexible probe may either contribute work to, or dissipate energy from, the system; black arrows denote the direction of travel around the cycle. Areas denoting positive work contributed by the probe are shaded in magenta, and those denoting dissipation from the probe are shaded in stippled green. For a driving stimulus of 3 Hz and 56 nm (top), W_{SF} = -217 zJ, with the stimulus fiber contributing positive work only at the positive extreme of the bundle's position (magenta area). W_D = -112 zJ, making W_A = +329 zJ. When the driving frequency was increased to 18 Hz (bottom), W_{SF} = +273 zJ, W_D = -270 zJ, giving W_A = -3 zJ. **B.** W_A calculated in response to 11 discrete stimulus frequencies at six amplitudes. The closed black arrow indicates the W_A value calculated from (**A**, top) and the open black arrow indicates that calculated from (**A**, bottom).

Finally, we observed that iontophoretic application of gentamicin impeded this frequency-tuned production of mechanical work. While the hair bundle was bathed in this drug and for all stimulus frequencies and amplitudes, we saw a striking absence of hair-bundle work production (Figure 4.3 A, B). Several minutes after turning off the iontophoretic current, W_A returned almost completely to baseline values, and frequency tuning resumed (Figure 4.3 C, D). In the hair bundle's recovery from the drug, we were surprised to see the development of negative values of W_A at higher frequencies of stimulation (Figure 4.3 D, right two-thirds of graph).

Including the cell whose data are shown in Figures 4.1 – 4.3, we obtained recordings from seven *L. appendix* hair cells that performed positive mechanical work comparable to, but often several-fold greater than, that produced by bullfrog saccular hair bundles (Martin and Hudspeth, 1999). Additionally, we successfully iontophoresed gentamicin onto four of these cells and observed their work production vanish; in three of these cells we were able to record a post-gentamicin recovery of work production. Furthermore, all seven recordings showed frequency dependence of work production; when driven more than a few hertz above their oscillation frequency, positive work production sharply declined.

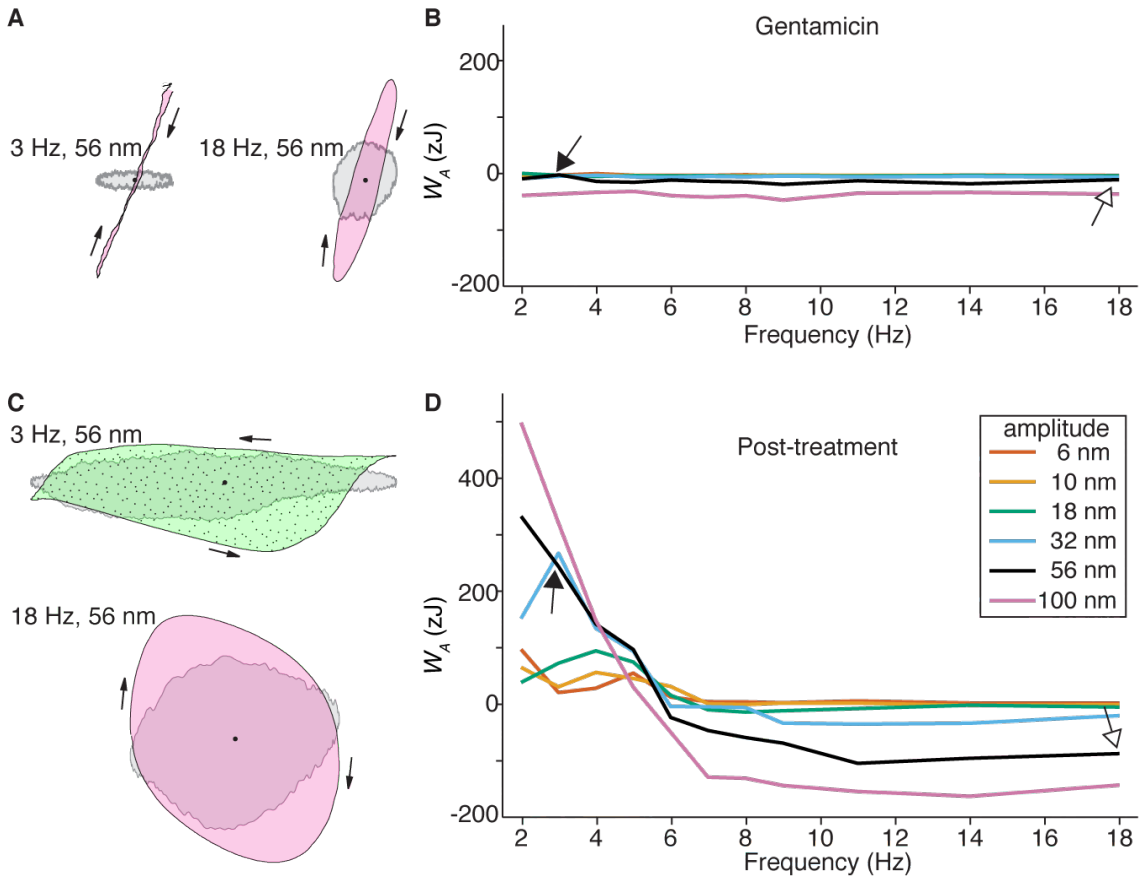

Figure 4.3. Frequency-tuned work production by *L. appendix* utricular hair bundles is reversibly abolished by gentamicin. A. During iontophoretic application of gentamicin, driving the stimulus fiber at 3 Hz and 56 nm yielded W_{SF} = +4 zJ, W_D = -6 zJ, giving W_A = -2 zJ (left). At 18 Hz and 56 nm, W_{SF} = +29 zJ, W_D = -22 zJ, making W_A = +7 zJ (right). **B.** W_A calculated for each driving frequency and amplitude in the presence of gentamicin. The closed black arrow indicates the W_A value calculated from (**A**, left) and the open black arrow indicates that calculated from (**A**, right). **C.** Several minutes after ceasing gentamicin iontophoresis, stimulation at 3 Hz and 56 nm gave W_{SF} = -147 zJ, W_D = -97 zJ, making W_A = -+244 zJ (top). The 18 Hz, 56 nm stimulus yielded W_{SF} = +238 zJ and W_D = -150 zJ, yielding W_A = -88 zJ (bottom). **D.** W_A calculated for each driving frequency and amplitude after gentamicin removal. The closed black arrow indicates the W_A value calculated from (**C**, top) and the open black arrow indicates that calculated from (**C**, bottom).

5. Discussion

Hair bundles are active participants in the process of sensory transduction. They expend chemical energy to perform work, and can harness this capability to amplify their mechanical response to a stimulus – loosely analogous to a child on a swing working to amplify an external push. The hair-bundle active process preferentially amplifies low-amplitude stimuli, compressing a million-fold range of sound amplitudes into a hundred-fold range of mechanical response (Hudspeth, 2008). This ability to entrain to and selectively amplify the weakest of tones allows an animal to detect vibrations of an amplitude comparable to that of thermally fluctuating water molecules. The active process is also tuned: for a given hair cell, a particular frequency elicits a mechanical gain much higher than do its flanking frequencies, a feature valuable in the analysis of complex sounds. Under some conditions, the hair bundle's state can cross a bifurcation into an unstable regime, at which point it undergoes spontaneous oscillations. All these traits, characteristic of an amplifier operating near a Hopf bifurcation, are seen in the behavior of the hair cells of tetrapod vertebrates. Although some tetrapod groups have derived an additional amplifying process (Fisher et al., 2012; Beurg et al., 2013) and some insects appear to have independently evolved an analogous amplifier (Warren et al., 2010), the hair-bundle active process is currently presumed unique to tetrapod vertebrates.

Every vertebrate, however, does have an inner ear populated with hair cells. Although some mechanical studies of teleost fish ears have suggested nonlinear amplification (Rabbitt et al., 2010), the question of amplification by the hair cells of non-tetrapod vertebrates has been largely ignored. We have therefore inquired whether the

active process had already evolved before the emergence of the tetrapods, and even the emergence of teleosts; is this perhaps a trait ancestral to all vertebrates?

When studying vertebrate "inventions," we often gain insights from the vertebrate group most distantly related to us: the jawless vertebrates, a clade whose extant members are hagfish and lampreys (Figure 1.9) (Blair and Hedges, 2005; Janvier, 2011). For example, the adaptive immune system is fundamentally similar among all jawed vertebrates, with the genes for T-cell receptors and B-cell receptors separated into the canonical rearranging segments, with common recombinase genes, and with conserved genes employed for antigen presentation. These similarities, maintained from sharks to chickens, imply that the origin of our adaptive immune system predates the radiation of jawed vertebrates (Cooper and Alder, 2006). Yet taking the smallest possible step in the basal direction, examining extant lampreys and hagfish, reveals a radically different but functionally analogous adaptive immune system. In jawless vertebrates, different genes are used to generate the staggeringly diverse antigen receptors forming the basis of adaptive immunity. But further investigations revealed that, despite these differences, jawless and jawed vertebrates both develop three lineages of immune lymphocytes (Hirano et al., 2014). Immunologists now face the surprising possibility that the fundamental organization of the immune system is ancestral to all vertebrates, with two independent strategies for antigen recognition that evolved later.

Because hair cells occur in all vertebrates, and even in members of their sister group (Burighel et al., 2003), we inquired whether the hair-bundle active process is ancestral to the entire vertebrate clade by investigating lampreys. If we found their hair cells to employ an amplifying ability, we wanted to know whether it was homologous or

analogous to the active process of tetrapods. Given that jawed and jawless vertebrates each radiated and evolved for 520 – 650 million years (Blair and Hedges, 2005) after their divergence, we accepted that even a homologous active process could have differing manifestations between these two groups.

We found that the utricular hair bundles of two lamprey species, *L. appendix* and *P. marinus*, displayed robust spontaneous oscillations. For both species, the oscillations bore a striking similarity to those from the bullfrog's sacculus in their regularity and in their display of two timescales (Figure 3.4). In other words, they resembled "relaxation oscillations," implying that something in these lamprey hair bundles slowly adjusts an internal parameter, driving the hair bundle to an instability that provokes a rapid lurch. Because we next wished to ascertain the likelihood that lamprey oscillations are homologous with tetrapod spontaneous oscillations, this initial mechanistic hint was heartening and instructive.

We focused on one species, *L. appendix*, and first explored the slow-timescale component of its spontaneous oscillations. Applying the model of tetrapod hair-bundle motility, we predicted that the slow, active driver of lamprey hair-bundle motility might be a form of myosin. As a potential effector of adaptation, this protein might be sensitive to feedback from the transduction channels. Not knowing the channels' conductance properties, we held a working assumption that as in tetrapods Ca^{2+} enters through channels and serves as this feedback signal. Our experimental manipulation of Ca^{2+} supported this; higher concentrations of extracellular Ca^{2+}, which increase the flux of this ion through open transduction channels, abbreviated the time an oscillating hair bundle spent deflected toward its taller edge. Furthermore, this effect was limited to the states

when transduction channels were expected to be open; extracellular Ca^{2+} had little effect on the time a hair bundle spent deflected toward its shorter edge (Figure 3.5). This result is consistent with intracellular Ca^{2+} feeding back on a myosin motor, promoting its slippage down stereociliary actin.

Our work with Ca^{2+} provided two general insights. First, the key role played by this cation in regulating hair-bundle dynamics is likely to be conserved throughout vertebrates. Second, the effects of this cation were consistent with a myosin acting as the driver of spontaneous oscillations in the lamprey. To further test the latter proposition, we employed known myosin blockers. Butanedione monoxime consistently abolished lamprey spontaneous oscillations in a manner that was often reversible. This drug has classically been used in studies of the bullfrog's hair cells, with a similar effect. Because tetrapod hair cells almost certainly employ myosin Ic as their adaptation motor, we also treated oscillating hair bundles from lamprey with a selective inhibitor of class I myosins called PClP. Although extracellular application of this drug rapidly halted spontaneous oscillations of hair bundles from the bullfrog, to our surprise it failed to halt these movements in the lamprey. Further work remains to be done to assure us that the drug indeed enters lamprey hair bundles. The adaptation motor of bullfrog hair bundles is affected dramatically within several minutes of applying 2.5 μM PClP, whereas lamprey hair bundles continue oscillating in four-fold higher concentrations of the drug for upwards of 30 minutes. It seems very unlikely that membrane permeabilities to this drug vary so extremely between these species. That lampreys and tetrapods seem to employ different classes of myosin as their adaptation motors affects the evolutionary interpretations of our study. This will be discussed in greater detail below.

Our findings at this point indicated that, as in tetrapods, the hair bundles of lampreys possess mechanotransduction channels whose collective gating creates negative bundle stiffness (Figure 1.6). The rapid jumps seen in lamprey spontaneous oscillations suggested this (Figure 1.8). And more specifically, that altering extracellular Ca^{2+} affected only the positive residence time suggests that these rapid jumps correlate with transitions between states of differing Ca^{2+} conductance. This finding implied that the rapid jumps were the mechanical result of concerted channel gating: jumps toward the positive edge represented channels snapping open, and negative-going jumps stemmed from channels slamming shut. To pursue this further, we employed a known blocker of tetrapod mechanotransduction channels, gentamicin. Applying this drug extracellularly reversibly halted lamprey spontaneous oscillations and did so in a concentration-dependent manner, biasing the hair bundle toward its taller edge. This result agreed with the mode of gentamicin's action on bullfrog hair bundles, in which the drug wedges channels in their open configuration while occluding their conductance pathway. Thus we gained evidence that the lamprey hair-cell mechanotransduction channels generate the mechanical instability required for relaxation oscillations and are sufficiently similar to gnathostome transduction channels to afford a sensitivity to gentamicin.

Spontaneous hair-bundle oscillations arise as an epiphenomenon of an active process that is capable of mechanically amplifying sinusoidal stimuli, endowing hair bundles with the ability to respond to weak inputs in a frequency-tuned manner (Martin and Hudspeth, 1999). Knowing this, we sought to determine whether spontaneous hair-bundle oscillations in the lamprey are associated with an ability to mechanically amplify sinusoidal stimuli. Indeed, we found that lamprey hair bundles can entrain to a periodic

stimulus and in so doing, contribute hundreds of zeptojoules of mechanical work to each cycle of motion. Comparing responses to stimuli of the same amplitude and of frequencies just below the preferred frequency of each bundle, we were intrigued to see that lamprey hair bundles could perform five times the mechanical work exerted by bullfrog hair bundles (Martin and Hudspeth, 1999). Perhaps a further investigation of the lamprey transduction apparatus can help explain the apparent brawn of lamprey hair bundles. As our understanding of energy dissipation in hair bundles continues to improve, we could alternately re-calculate work production by lamprey and bullfrog hair bundles with improved estimates of hydrodynamic drag coefficients. These improved estimates can be calculated from the Brownian motion of both species' hair bundles after cleaving tip links; after decoupling bundle motion from internal viscoelastic elements, non-hydrodynamic sources of dissipation can be ignored. Viscoelastic contributions were originally considered to be dwarfed by hydrodynamics (Denk et al., 1989; Martin and Hudspeth, 1999), but recent analyses of bullfrog hair bundles (Bormuth et al., 2014) suggest that the hydrodynamic drag coefficient used in the calculation of active work by sinusoidally driven bullfrog hair bundles had been overestimated by roughly 50%. Addressing this in both bullfrog and lamprey will facilitate direct comparison between work production in these disparate species.

Given these data, our view is that the active process likely existed in the ancestor to all vertebrates. However, an alternate scenario remains possible – that the active process evolved more than once in the vertebrates, and the lamprey active process can be regarded as analogous to that of tetrapods. We consider this explanation less parsimonious, especially in light of the functional similarities between this trait in the two

groups. But there are reasons to maintain the possibility of convergent evolution. First, our findings with the class I myosin inhibitor PClP suggest that different classes of myosins are employed as the adaptation motors in the two groups. With this mechanistic difference in mind, we can imagine a stepwise evolution of the active process (Hudspeth, 2008). Maybe hair cells in the ancestor to jawed and jawless vertebrates lacked one ingredient of the active process, having no adaptation motors, or having adaptation motors that were insensitive to Ca^{2+} entry from transduction channels (Choe et al., 1998). We could grant that this ancestral hair cell possessed the second ingredient of the active process, negative stiffness (Figure 1.6). Though not obviously adaptive on its own, negative stiffness can emerge from the gating of mechanotransduction channels. It seems possible that the hair bundles of jawless and jawed vertebrates retained this plesiomorphic state, but at some point each independently incorporated a Ca^{2+}-sensitive myosin motor into its transduction apparatus.

A second reason to not reject the possibility of convergent evolution between the two clades is that we could have more widely sampled the extant members of these groups. The two species of lamprey we examined, *L. appendix* and *P. marinus*, share a relatively recent common ancestor that existed 10 – 40 million years ago (Kuraku and Kuratani, 2006), whereas the rift between jawed and jawless vertebrates occurred in the much more distant past, around 600 million years ago (Blair and Hedges, 2005). Although describing spontaneous oscillations in two lamprey species bolsters our claim that the active process is ancestral to all vertebrates, the relative closeness of these species is a weakness. The 550 million years between the jawed-jawless node and the *Lampetra-Petromyzon* node afforded considerable time for evolutionary change to take

place, reducing the utility of the parsimony employed in the preceding paragraph. To address this, we suggest examining the inner-ear hair bundles of the pouched lamprey *Geotria australis*, a resident of the southern hemisphere. This species diverged from the two species used in this study 220 – 280 million years ago (Kuraku and Kuratani, 2006). Another valuable pursuit would be looking for hair-bundle motility in a species of the hagfish, whose most recent ancestor shared with the lamprey existed 430 – 520 million years ago (Blair and Hedges, 2005; Kuraku and Kuratani, 2006).

In jawed fish, the ancestral mode of acoustic perception is thought to be near-field hearing, or the perception of oscillating hydrodynamic flows from a vibrating source (Figure 1.4, left column). Because the spatial extent of the acoustic near field is proportional to the wavelength of a sound, low-frequency tones are the most useful stimuli emanating from a distant sound source for these hearing "generalists." Our finding that the lamprey's utricular hair bundles preferentially amplify tones below 10 Hz may be related to this fact. Furthermore, the sound amplitude in the acoustic near field decays as steeply as $1/r^3$ in relation to the distance r from the source (Fay and Popper, 1999). We might therefore expect amplification of very faint vibrations to be of use when an animal must detect a distant stimulus, as might be the case for an adult parasitic lamprey seeking a teleost host.

It may also be important for lamprey to detect self-generated movements of their own body to provide feedback to motor systems. For example, swimming by lampreys entails significant oscillations of the head in the horizontal plane, and their ocular muscles are capable of adjusting eye position in the same plane (Maklad et al., 2014). The detection of head motion may therefore influence the activity of these muscles.

Loaded with an overlying otolithic mass, the utricular hair cells may be poised to detect head vibrations through the same mode posited for near-field sound detection: vibrations of the fish are lagged by vibrations of the inertial mass, deflecting hair bundles (Figure 1.4). Furthermore, the periodic horizontal motion of the head of a swimming lamprey occurs at several hertz, near the stimulus frequency provoking peak work production by utricular hair cells (Figure 4.2). It would be interesting to further explore this issue, which could represent the first time the active process has been implicated in sensorimotor feedback.

Our finding that the active process likely evolved before the evolution of jaws may help us better understand the evolutionary history of vertebrates. This observation suggests that, in the absence of secondary losses, the hair bundles of cartilaginous fish, sturgeons, and ray-finned fish probably all display this active process. This may especially inform our view of the hearing "specialists," such as catfish, that have evolved peripheral mechanisms for detecting far field sound in water (Figure 1.4, right column). In this group, far-field hearing is thought to have evolved under pressures to detect high-frequency sounds, the sensory transduction of which is particularly antagonized by hydrodynamic drag (Hudspeth, 2014). Our study is the first to afford an initial presumption that the ancestors to these hearing specialists had an active process to counter the dissipative effects of drag, giving high-frequency sounds some chance to be transduced. Against the backdrop of this symplesiomorphy, it is easier to imagine how peripheral mechanisms of far-field reception could have been selectively advantageous. This speculative extension of our findings into the teleost group indicates how the new insights of our study can be applied to studying the history of vertebrates and their ears.

References

Adamson, S. L., Lu, Y., Whiteley, K. J., Holmyard, D., Hemberger, M., Pfarrer, C. and Cross, J. C. (2002) 'Interactions Between Trophoblast Cells and the Maternal and Fetal Circulation in the Mouse Placenta', *Developmental Biology*, **250**, 358–373.

Aisenberg, A. and Barrantes, G. (2011) 'Sexual Behavior, Cannibalism, and Mating Plugs as Sticky Traps in the Orb Weaver Spider Leucauge Argyra (Tetragnathidae)', *Naturwissenschaften*, **98**, 605–613.

Arch, V. S., Grafe, T. U., Gridi-Papp, M. and Narins, P. M. (2009) 'Pure Ultrasonic Communication in an Endemic Bornean Frog.', *PloS one*, **4**, e5413.

Arkley, K., Grant, R. A., Mitchinson, B. and Prescott, T. J. (2014) 'Strategy Changein Vibrissal Active Sensing During Rat Locomotion', *Current Biology*, **24**, 1507–1512.

Ayala, F. J., Rzhetsky, A. and Ayala, F. J. (1998) 'Origin of the Metazoan Phyla: Molecular Clocks Confirm Paleontological Estimates.', *Proceedings Of The National Academy Of Sciences Of The United States Of America*, **95**, 606–611.

Baker, M. A. (1982) 'Brain Cooling in Endotherms in Heat and Exercise.', *Annual Review of Physiology*, **44**, 85–96.

Baldwin, M. W., Toda, Y., Nakagita, T., O'Connell, M. J., Klasing, K. C., Misaka, T., Edwards, S. V. and Liberles, S. D. (2014) 'Sensory Biology. Evolution of Sweet Taste Perception in Hummingbirds by Transformation of the Ancestral Umami Receptor.', *Science*, **345**, 929–933.

Benser, M., Marquis, R. E. and Hudspeth, A. J. (1996) 'Rapid, Active Hair Bundle Movements in Hair Cells From the Bullfrog's Sacculus', *The Journal of Neuroscience*, **16**, 5629–5643.

Beuchat, C. A. (1990) 'Body Size, Medullary Thickness, and Urine Concentrating Ability in Mammals.', *The American Journal of Physiology*, **258**, R298–308.

Beurg, M., Fettiplace, R., Nam, J.-H. and Ricci, A. J. (2009) 'Localization of Inner Hair Cell Mechanotransducer Channels Using High-Speed Calcium Imaging', *Nature Neuroscience*, **12**, 553–558.

Beurg, M., Tan, X. and Fettiplace, R. (2013) 'A Prestin Motor in Chicken Auditory Hair Cells: Active Force Generation in a Nonmammalian Species', *Neuron*, **79**, 69–81.

Blair, J. E. and Hedges, S. B. (2005) 'Molecular Phylogeny and Divergence Times of Deuterostome Animals.', *Molecular Biology And Evolution*, **22**, 2275–2284.

Blair, W. F. (1964) 'Isolating Mechanisms and Interspecies Interactions in Anuran Amphibians', *The Quarterly Review of Biology*, **39**, 334–344.

Boekhoff-Falk, G. (2005) 'Hearing in Drosophila: Development of Johnston's Organ and Emerging Parallels to Vertebrate Ear Development', *Developmental Dynamics*, **232**, 550–558.

Bormuth, V., Barral, J., Joanny, J. F., Jülicher, F. and Martin, P. (2014) 'Transduction Channels' Gating Can Control Friction on Vibrating Hair-Cell Bundles in the Ear', *Proceedings of the National Academy of Sciences*, **111**, 7185–7190.

Bosher, S. and Warren, R. (1968) 'Observations on the Electrochemistry of the Cochlear Endolymph of the Rat: a Quantitative Study of Its Electrical Potential and Ionic Composition as Determined by Means of Flame Spectrophotometry', *Proceedings Of The Royal Society Of London Series B-Biological Sciences*, **171**, 227–247.

Bosher, S. and Warren, R. (1978) 'Very Low Calcium Content of Cochlear Endolymph, an Extracellular Fluid', *Nature*, **273**, 377–378.

Bozovic, D. and Hudspeth, A. J. (2003) 'Hair-Bundle Movements Elicited by Transepithelial Electrical Stimulation of Hair Cells in the Sacculus of the Bullfrog.', *Proceedings Of The National Academy Of Sciences Of The United States Of America*, **100**, 958–963.

Burighel, P., Caicci, F. and Manni, L. (2011) 'Hair Cells in Non-Vertebrate Models: Lower Chordates and Molluscs', *Hearing Research*, **273**, 14-24.

Burighel, P., Lane, N. J., Fabio, G., Stefano, T., Zaniolo, G., Carnevali, M. D. C. and Manni, L. (2003) 'Novel, Secondary Sensory Cell Organ in Ascidians: in Search of the Ancestor of the Vertebrate Lateral Line.', *The Journal of Comparative Neurology*, **461**, 236–249.

Caicci, F., Degasperi, V., Gasparini, F., Zaniolo, G., Del Favero, M., Burighel, P. and Manni, L. (2010) 'Variability of Hair Cells in the Coronal Organ of Ascidians (Chordata, Tunicata)', *Canadian Journal of Zoology*, **88**, 567–578.

Carey, F. G. and Teal, J. M. (1966) 'Heat Conservation in Tuna Fish Muscle', *Proceedings Of The National Academy Of Sciences Of The United States Of America*, **56**, 1464.

Cator, L. J., Arthur, B. J., Harrington, L. C. and Hoy, R. R. (2009) 'Harmonic Convergence in the Love Songs of the Dengue Vector Mosquito.', *Science*, **323**, 1077–1079.

Chang, C.-H. and Davies, J. A. (2012) 'An Improved Method of Renal Tissue Engineering, by Combining Renal Dissociation and Reaggregation with a Low-Volume Culture Technique, Results in Development of Engineered Kidneys Complete with Loops of Henle', *Nephron Experimental Nephrology*, **121**, e79–e85.

Cheung, E. and Corey, D. (2006) 'Ca2+ Changes the Force Sensitivity of the Hair-Cell Transduction Channel', *Biophysical Journal*, **90**, 124–139.

Chinthalapudi, K., Taft, M. H., Martin, R., Heissler, S. M., Preller, M., Hartmann, F. K., Brandstaetter, H., Kendrick-Jones, J., Tsiavaliaris, G., Gutzeit, H. O., Fedorov, R., Buss, F., Knolker, H. J., Coluccio, L. M. and Manstein, D. J. (2011) 'Mechanism and Specificity of Pentachloropseudilin-Mediated Inhibition of Myosin Motor Activity', *Journal Of Biological Chemistry*, **286**, 29700–29708.

Chittka, L., Thomson, J. D. and Waser, N. M. (1999) 'Flower Constancy, Insect Psychology, and Plant Evolution', *Naturwissenschaften*, **86**, 361–377.

Choe, Y., Magnasco, M. and Hudspeth, A. J. (1998) 'A Model for Amplification of Hair-Bundle Motion by Cyclical Binding of Ca2+ to Mechanoelectrical-Transduction Channels', *Proceedings Of The National Academy Of Sciences Of The United States Of America*, **95**, 15321.

Cooper, M. D. and Alder, M. N. (2006) 'The Evolution of Adaptive Immune Systems', *Cell*, **124**, 815–822.

Corey, D. and Hudspeth, A. J. (1983) 'Kinetics of the Receptor Current in Bullfrog Saccular Hair-Cells', *The Journal of Neuroscience*, **3**, 962–976.

Crawford, A. and Fettiplace, R. (1985) 'The Mechanical Properties of Ciliary Bundles of Turtle Cochlear Hair Cells.', *The Journal of Physiology*, **364**, 359–379.

Crawford, A. C., Evans, M. G. and Fettiplace, R. (1991) 'The Actions of Calcium on the Mechano-Electrical Transducer Current of Turtle Hair Cells.', *The Journal of Physiology*, **434**, 369–398.

Cyr, J. L., Dumont, R. A. and Gillespie, P. G. (2002) 'Myosin-1c Interacts with Hair-Cell Receptors Through Its Calmodulin-Binding IQ Domains.', *The Journal of Neuroscience*, **22**, 2487–2495.

Denk, W., Webb, W. and Hudspeth, A. J. (1989) 'Mechanical Properties of Sensory Hair Bundles Are Reflected in Their Brownian Motion Measured with a Laser Differential Interferometer', *Proceedings Of The National Academy Of Sciences Of The United States Of America*, **86**, 5371–5375.

Eatock, R. A., Corey, D. P. and Hudspeth, A. J. (1987) 'Adaptation of Mechanoelectrical Transduction in Hair Cells of the Bullfrog's Sacculus.', *The Journal of Neuroscience*, **7**, 2821–2836.

Engelmann, J., Hanke, W., Mogdans, J. and Bleckmann, H. (2000) 'Hydrodynamic Stimuli and the Fish Lateral Line.', *Nature*, **408**, 51–52.

Enger, P. S. and Andersen, R. (1967) 'An Electrophysiological Field Study of Hearing in Fish.', *Comparative Biochemistry and Physiology*, **22**, 517–525.

Fay, R. R. and Popper, A. N. (1999) *Comparative Hearing: Fish and Amphibians*, New York, NY, Springer Science & Business Media.

Fisher, J. A. N., Nin, F., Reichenbach, T., Uthaiah, R. C. and Hudspeth, A. J. (2012) 'The Spatial Pattern of Cochlear Amplification', *Neuron*, **76**, 989–997.

Francis, E. and Horton, F. M. (1936) 'Some Reactions of the Ammocoete', *The Journal of Experimental Biology*, **13**, 410–415.

Gillespie, P. G. and Cyr, J. L. (2004) 'Myosin-1c, the Hair Cell's Adaptation Motor', *Annual Review of Physiology*, **66**, 521–545.

Gould, S. and Lewontin, R. (1979) 'The Spandrels of San Marco and the Panglossian Paradigm: a Critique of the Adaptationist Programme', *Proceedings Of The Royal Society Of London Series B-Biological Sciences*, **205**, 581.

Grant, V. (1949) 'Pollination Systems as Isolating Mechanisms in Angiosperms.', *Evolution*, **3**, 82–97.

Hammond, K. and Whitfield, T. (2006) 'The Developing Lamprey Ear Closely Resembles the Zebrafish Otic Vesicle: Otx1 Expression Can Account for All Major Patterning Differences', *Development*, **133**, 1347–1357.

Hardie, R. C., Martin, F., Cochrane, G. W., Juusola, M., Georgiev, P. and Raghu, P. (2002) 'Molecular Basis of Amplification in Drosophila Phototransduction: Roles for G Protein, Phospholipase C, and Diacylglycerol Kinase.', *Neuron*, **36**, 689–701.

Hargitay, B. and Kuhn, W. (2001) 'The Multiplication Principle as the Basis for Concentrating Urine in the Kidney', *Journal of the American Society of Nephrology,* **12**, 1566 - 1586.

Harrington, M. J. and Waite, J. H. (2007) 'Holdfast Heroics: Comparing the Molecular and Mechanical Properties of Mytilus Californianus Byssal Threads', *Journal of Experimental Biology*, **210**, 4307–4318.

Herrmann, C., Wray, J., Travers, F. and Barman, T. (1992) 'Effect of 2,3-Butanedione Monoxime on Myosin and Myofibrillar ATPases. an Example of an Uncompetitive Inhibitor.', *Biochemistry*, **31**, 12227–12232.

Hill, R. W., Wyse, G. A. and Anderson, M. (2012) *Animal Physiology*, Sunderland, MA, Sinauer Associates Incorporated.

Hirano, M., Guo, P., McCurley, N., Schorpp, M., Das, S., Boehm, T. and Cooper, M. D. (2014) 'Evolutionary Implications of a Third Lymphocyte Lineage in Lampreys', *Nature*, **501**, 435–438.

Holt, J., Gillespie, S., Provance, D., Jr, Shah, K., Shokat, K., Corey, D., Mercer, J. and Gillespie, P. G. (2002) 'A Chemical-Genetic Strategy Implicates Myosin-1c in Adaptation by Hair Cells', *Cell*, **108**, 371–381.

Howard, J. and Hudspeth, A. J. (1988) 'Compliance of the Hair Bundle Associated with Gating of Mechanoelectrical Transduction Channels in the Bullfrog's Saccular Hair Cell', *Neuron*, **1**, 189–199.

Hudspeth, A. J. (2008) 'Making an Effort to Listen: Mechanical Amplification in the Ear', *Neuron*, **59**, 530–545.

Hudspeth, A. J. (2014) 'Integrating the Active Process of Hair cells with Cochlear Function', *Nature Publishing Group*, **15**, 600–614.

Hudspeth, A. J. and Gillespie, P. G. (1994) 'Pulling Springs to Tune Transduction-Adaptation by Hair Cells', *Neuron*, **12**, 1–9.

Ingber, D. E. (2002) 'Mechanical Signaling and the Cellular Response to Extracellular Matrix in Angiogenesis and Cardiovascular Physiology', *Circulation Research*, **91**, 877–887.

Janvier, P. (2011) 'Comparative Anatomy: All Vertebrates Do Have Vertebrae', *Current Biology*, **21**, R661–R663.

Jaramillo, F. and Hudspeth, A. J. (1991) 'Localization of the Hair Cell"S Transduction Channels at the Hair Bundle"s Top by Iontophoretic Application of a Channel Blocker.', *Neuron*, **7**, 409–420.

Jensen-Smith, H. C., Eley, J., Steyger, P. S., Ludueña, R. F. and Hallworth, R. (2003) 'Cell Type-Specific Reduction of Beta Tubulin Isotypes Synthesized in the Developing Gerbil Organ of Corti.', *Journal of Neurocytology*, **32**, 185–197.

Johnsen, H. K., Blix, A. S., Jørgensen, L. and Mercer, J. B. (1985) 'Vascular Basis for Regulation of Nasal Heat Exchange in Reindeer.', *The American Journal of Physiology*, **249**, R617–23.

Johnsen, S. and Lohmann, K. J. (2005) 'The Physics and Neurobiology of Magnetoreception', *Nature Publishing Group*, **6**, 703–712.

Karavitaki, K. D. and Corey, D. P. (2010) 'Sliding Adhesion Confers Coherent Motion to Hair Cell Stereocilia and Parallel Gating to Transduction Channels.', *The Journal of Neuroscience*, **30**, 9051–9063.

Katori, Y., Takasaka, T., Ishikawa, M. and Tonosaki, A. (1994) 'Fine Structure and Lectin Histochemistry of the Apical Surface of the Free Neuromast of Lampetra Japonica', *Cell and Tissue Research*, **276**, 245–252.

Kay, K. M. and Sargent, R. D. (2009) 'The Role of Animal Pollination in Plant Speciation: Integrating Ecology, Geography, and Genetics', *Annual Review of Ecology, Evolution, and Systematics*, **40**, 637–656.

Kozlov, A. S., Risler, T. and Hudspeth, A. J. (2007) 'Coherent Motion of Stereocilia Assures the Concerted Gating of Hair-Cell Transduction Channels', *Nature Neuroscience*, **10**, 87–92.

Kroder, S., Samietz, J. and Dorn, S. (2006) 'Effect of Ambient Temperature on Mechanosensory Host Location in Two Parasitic Wasps of Different Climatic Origin', *Physiological Entomology*, **31**, 299–305.

Kuraku, S. and Kuratani, S. (2006) 'Time Scale for Cyclostome Evolution Inferred with a Phylogenetic Diagnosis of Hagfish and Lamprey cDNA Sequences', *Zoological Science*, **23**, 1053–1064.

Le Goff, L., Bozovic, D. and Hudspeth, A. J. (2005) 'Adaptive Shift in the Domain of Negative Stiffness During Spontaneous Oscillation by Hair Bundles From the Internal Ear', *Proceedings of the National Academy of Sciences*, **102**, 16996.

Lewis, E. R. (1981) 'Evolution of Inner-Ear Auditory Apparatus in the Frog.', *Brain Research*, **219**, 149–155.

Lohmann, K. J. (2010) 'Q&A: Animal Behaviour: Magnetic-Field Perception', *Nature*, **464**, 1140–1142.

Low, S. E., Amburgey, K., Horstick, E., Linsley, J., Sprague, S. M., Cui, W. W., Zhou, W., Hirata, H., Saint-Amant, L., Hume, R. I. and Kuwada, J. Y. (2011) 'TRPM7 Is Required Within Zebrafish Sensory Neurons for the Activation of Touch-Evoked Escape Behaviors', *The Journal of Neuroscience,* **31**, 11633–11 644.

Lowenstein, O. (1970) 'The Electrophysiological Study of the Responses of the Isolated Labyrinth of the Lamprey (Lampetra Fluviatilis) to Angular Acceleration, Tilting and Mechanical Vibration', *Proceedings Of The Royal Society Of London Series B-Biological Sciences*, **174**, 419–434.

Lowenstein, O. and Compton, G. J. (1978) 'A Comparative Study of the Responses of Isolated First-Order Semicircular Canal Afferents to Angular and Linear Acceleration, Analysed in the Time and Frequency Domains', *Proceedings Of The Royal Society B-Biological Sciences*, **202**, 313–338.

Lowenstein, O. and Thornhill, R. (1970) 'The Labyrinth of Myxine: Anatomy, Ultrastructure and Electrophysiology', *Proceedings Of The Royal Society Of London Series B-Biological Sciences*, **176**, 21–42.

Lowenstein, O., Osborne, M. and Thornhill, R. (1968) 'The Anatomy and Ultrastructure of the Labyrinth of the Lamprey (Lampetra Fluviatilis L.)', *Proceedings Of The Royal Society Of London Series B-Biological Sciences*, **170**, 113.

Lumpkin, E. A., Marquis, R. E. and Hudspeth, A. J. (1997) 'The Selectivity of the Hair Cell's Mechanoelectrical-Transduction Channel Promotes Ca2+ Flux at Low Ca2+ Concentrations.', *Proceedings Of The National Academy Of Sciences Of The United States Of America*, **94**, 10997–11002.

Lumpkin, E. A., Marshall, K. L. and Nelson, A. M. (2010) 'Review Series: the Cell Biology of Touch', *The Journal of Cell Biology*, **191**, 237–248.

Mackie, G., Burighel, P., Caicci, F. and Manni, L. (2006) 'Innervation of Ascidian Siphons and Their Responses to Stimulation', *Canadian Journal of Zoology*, **84**, 1146–1162.

Maklad, A., Reed, C., Johnson, N. S. and Fritzsch, B. (2014) 'Anatomy of the Lamprey Ear: Morphological Evidence for Occurrence of Horizontal Semicircular Ducts in the Labyrinth of Petromyzon Marinus', *Journal of Anatomy*, **224**, 432–446.

Manley, G. A., Sienknecht, U. and Köppl, C. (2004) 'Calcium Modulates the Frequency and Amplitude of Spontaneous Otoacoustic Emissions in the Bobtail Skink.', *Journal Of Neurophysiology*, **92**, 2685–2693.

Manni, L., Caicci, F., Gasparini, F., Zaniolo, G. and Burighel, P. (2004) 'Hair Cells in Ascidians and the Evolution of Lateral Line Placodes.', *Evolution & development*, **6**, 379–381.

Martin, P. (2008) 'Active Hair-Bundle Motility of the Hair Cells of Vestibular and Auditory Organs'. In Manley, G. A., Fay, R. R., and Popper, A. N. (eds) *Active Processes and Otoacoustic Emissions*, New York, Springer, pp. 93–143.

Martin, P. and Hudspeth, A. J. (1999) 'Active Hair-Bundle Movements Can Amplify a Hair Cell's Response to Oscillatory Mechanical Stimuli', *Proceedings Of The National Academy Of Sciences Of The United States Of America*, **96**, 14306–14311.

Martin, P., Bozovic, D., Choe, Y. and Hudspeth, A. J. (2003) 'Spontaneous Oscillation by Hair Bundles of the Bullfrog's Sacculus.', *The Journal of neuroscience : the official journal of the Society for Neuroscience*, **23**, 4533–4548.

Martin, P., Mehta, A. D. and Hudspeth, A. J. (2000) 'Negative Hair-Bundle Stiffness Betrays a Mechanism for Mechanical Amplification by the Hair Cell', *Proceedings Of The National Academy Of Sciences Of The United States Of America*, **97**, 12026–12031.

Montealegre-Z, F., Jonsson, T., Robson-Brown, K. A., Postles, M. and Robert, D. (2012) 'Convergent Evolution Between Insect and Mammalian Audition.', *Science*, **338**, 968–971.

Nadrowski, B., Albert, J. T. and Goepfert, M. C. (2008) 'Transducer-Based Force Generation Explains Active Process in Drosophila Hearing', *Current Biology*, **18**, 1365–1372.

Newman, E., Manning, J. and Anderson, B. (2014) 'Matching Floral and Pollinator Traits Through Guild Convergence and Pollinator Ecotype Formation', *Annals of Botany*, **113**, 373–384.

Nicholson, C. (1993) 'Ion-Selective Microelectrodes and Diffusion Measurements as Tools to Explore the Brain Cell Microenvironment.', *Journal of Neuroscience Methods*, **48**, 199–213.

Nilsson, D. E. (2009) 'The Evolution of Eyes and Visually Guided Behaviour', *Philosophical Transactions of the Royal Society B: Biological Sciences*, **364**, 2833–2847.

Obholzer, N., Wolfson, S., Trapani, J. G., Mo, W., Nechiporuk, A., Busch-Nentwich, E., Seiler, C., Sidi, S., Sollner, C., Duncan, R. N., Boehland, A. and Nicolson, T. (2008) 'Vesicular Glutamate Transporter 3 Is Required for Synaptic Transmission in Zebrafish Hair Cells', *The Journal of Neuroscience,* **28**, 2110–2118.

Odell, G. M., Oster, G., Alberch, P. and Burnside, B. (1981) 'The Mechanical Basis of Morphogenesis. I. Epithelial Folding and Invagination.', *Developmental Biology*, **85**, 446–462.

Peter, C. I. and Johnson, S. D. (2014) 'A Pollinator Shift Explains Floral Divergence in an Orchid Species Complex in South Africa', *Annals of Botany*, **113**, 277–288.

Pfennig, K. S. (2000) 'Female Spadefoot Toads Compromise on Mate Quality to Ensure Conspecific Matings', *Behavioral Ecology*, **11**, 220–227.

Pippard, A. B. (2007) *The Physics of Vibration*, Cambridge University Press.

Poinar, G. O. and Hess, R. (1982) 'Ultrastructure of 40-Million-Year-Old Insect Tissue', *Science*, **215**, 1241–1242.

Popper, A. N. (1981) 'Comparative Scanning Electron Microscopic Investigations of the Sensory Epithelia in the Teleost Sacculus and Lagena.', *The Journal of Comparative neurology*, **200**, 357–374.

Purves, R. D. (1979) 'The Physics of Iontophoretic Pipettes.', *Journal of Neuroscience Methods*, **1**, 165–178.

Purves, R. D. (1981) *Microelectrode Methods for Intracellular Recording and Ionophoresis*, London, Academic Press.

Rabbitt, R. D., Boyle, R. and Highstein, S. M. (2010) 'Mechanical Amplification by Hair Cells in the Semicircular Canals', *Proceedings Of The National Academy Of Sciences Of The United States Of America*, **107**, 3864–3869.

Ricci, A. J., Crawford, A. and Fettiplace, R. (2000) 'Active Hair Bundle Motion Linked to Fast Transducer Adaptation in Auditory Hair Cells', *The Journal of Neuroscience*, **20**, 7131–7142.

Ricci, A. J., Crawford, A. and Fettiplace, R. (2002) 'Mechanisms of Active Hair Bundle Motion in Auditory Hair Cells', *The Journal of Neuroscience*, **22**, 44–52.

Richards, C. L. (2006) 'Has the Evolution of Complexity in the Amphibian Papilla Influenced Anuran Speciation Rates?', *Journal of Evolutionary Biology*, **19**, 1222–1230.

Rovner, J. S. and Barth, F. G. (1981) 'Vibratory Communication Through Living Plants by a Tropical Wandering Spider.', *Science*, **214**, 464–466.

Ruggero, M., Rich, N., Recio, A., Shyamla Narayan, S. and Robles, L. (1997) 'Basilar-Membrane Responses to Tones at the Base of the Chinchilla Cochlea', *Acoustical Society of America*, **101**, 2151–2163.

Runhaar, G. and Manley, G. A. (1987) 'Potassium Concentration in the Inner Sulcus Is Perilymph-Like.', *Hearing Research*, **29**, 93–103.

Rüsch, A. and Thurm, U. (1990) 'Spontaneous and Electrically Induced Movements of Ampullary Kinocilia and Stereovilli', *Hearing Research*, **48**, 247–264.

Ryan, M. J. (1986) 'Neuroanatomy Influences Speciation Rates Among Anurans.', *Proceedings Of The National Academy Of Sciences Of The United States Of America*, **83**, 1379–1382.

Ryan, M. J. and Rand, A. S. (1995) 'Female Responses to Ancestral Advertisement Calls in Tungara Frogs.', *Science*, **269**, 390–392.

Schwarz, J. S., Reichenbach, T. and Hudspeth, A. J. (2011) 'A Hydrodynamic Sensory Antenna Used by Killifish for Nocturnal Hunting.', *Journal of Experimental Biology*, **214**, 1857–1866.

Seehausen, O., van Alphen, J. J. and Witte, F. (1997) 'Cichlid Fish Diversity Threatened by Eutrophication That Curbs Sexual Selection', *Science*, **277**, 1808–1811.

Shlomovitz, R., Fredrickson-Hemsing, L., Kao, A., Meenderink, S. W. F., Bruinsma, R. and Bozovic, D. (2013) 'Low Frequency Entrainment of Oscillatory Bursts in Hair Cells', *Biophysj*, **104**, 1661–1669.

Smith, E. F. (2002) 'Regulation of Flagellar Dynein by Calcium and a Role for an Axonemal Calmodulin and Calmodulin-Dependent Kinase.', *Molecular Biology of the Cell*, **13**, 3303–3313.

Söllner, C., Rauch, G.-J., Siemens, J., Geisler, R., Schuster, S. C., Müller, U., Nicolson, T.Tübingen 2000 Screen Consortium (2004) 'Mutations in Cadherin 23 Affect Tip Links in Zebrafish Sensory Hair Cells.', *Nature*, **428**, 955–959.

Strogatz, S. H. (1994) *Nonlinear Dynamics and Chaos*, Reading, MA, Addison-Wesley.

Tinevez, J., Jülicher, F. and Martin, P. (2007) 'Unifying the Various Incarnations of Active Hair-Bundle Motility by the Vertebrate Hair Cell', *Biophysical Journal*, **93**, 4053–4067.

van Netten, S. and Khanna, S. (1994) 'Stiffness Changes of the Cupula Associated with the Mechanics of Hair Cells in the Fish Lateral Line.', *Proceedings Of The National Academy Of Sciences Of The United States Of America*, **91**, 1549–1553.

Vogel, S. (1996) *Life in Moving Fluids*, Princeton, NJ, Princeton University Press.

Walker, R. and Hudspeth, A. J. (1996) 'Calmodulin Controls Adaptation of Mechanoelectrical Transduction by Hair Cells of the Bullfrog's Sacculus', *Proceedings Of The National Academy Of Sciences Of The United States Of America*, **93**, 2203–2207.

Warren, B., Lukashkin, A. N. and Russell, I. (2010) 'The Dynein–Tubulin Motor Powers Active Oscillations and Amplification in the Hearing Organ of the Mosquito', *Proceedings Of The Royal Society B-Biological Sciences*, **277**, 1761–1769.

Wilson, M. (2013) 'Ultrasonic Predator–Prey Interactions in Water–Convergent Evolution with Insects and Bats in Air?', *Frontiers in Physiology*, **137**, 1–12.

Wu, Y. C., Ricci, A. J. and Fettiplace, R. (1999) 'Two Components of Transducer Adaptation in Auditory Hair Cells.', *Journal Of Neurophysiology*, **82**, 2171–2181.